Quaternary Science Reviews 147 (2016) 178–193

Contents lists available at ScienceDirect

Quaternary Science Reviews

journal homepage: www.elsevier.com/locate/quascirev

Evolution of a high-latitude sediment drift inside a glacially-carved trough based on high-resolution seismic stratigraphy (Kveithola, NW Barents Sea)

Michele Rebesco [a, *], Asli Özmaral [b], Roger Urgeles [c], Daniela Accettella [a], Renata G. Lucchi [a], Denise Rüther [d, e], Monica Winsborrow [d], Jaume Llopart [c], Andrea Caburlotto [a], Hendrik Lantzsch [b], Till J.J. Hanebuth [b, f]

[a] OGS, Sgonico, TS, Italy
[b] MARUM—Center for Marine Environmental Sciences, Bremen, Germany
[c] Institut de Ciències del Mar, CSIC, Barcelona, Spain
[d] CAGE – Centre for Arctic Gas Hydrate, Environment and Climate, Department of Geology, UiT The Arctic University of Norway, Tromsø, Norway
[e] Faculty of Engineering and Science, Sogn og Fjordane University College, Sogndal, Norway
[f] School of Coastal and Marine Systems Science, Coastal Carolina University, Conway/SC, USA

ARTICLE INFO

Article history:
Received 3 July 2015
Received in revised form
24 January 2016
Accepted 5 February 2016
Available online 2 March 2016

Keywords:
Contourite drift
Moat
Glacial trough
Bottom currents
Brine-enriched shelf water
Contourites
Seismostratigraphy
Multibeam
Kveithola
Barents sea

ABSTRACT

Kveithola is a glacially-carved, E-W trending trough located in the NW Barents Sea, an epicontinental shelf sea of the Arctic Ocean located off northern Norway and Russia. A set of confined sediment drifts (the "Kveithola Drift") is located in the inner part of the trough. In general, drift deposits are commonly characterized by high lateral continuity, restricted occurrence of hiatuses and relatively high accumulation rates, and thus represent excellent repositories of paleo-environmental information. We provide for the first time a detailed morphological and seismostratigraphic insight into this sediment drift, which is further supported by some preliminary lithological and sedimentological analyses. The complex morphology of the drift, imaged by combining all available multibeam data, includes a main and a minor drift body, two drift lenses in the outer part of the trough, more or less connected drift patches in the innermost part and small perched sediment patches in a structurally-controlled channel to the north. The seismic (PARASOUND) data show that the main and minor drift bodies are mainly well-stratified, characterized by sub-parallel reflections of moderate to high amplitude and good lateral continuity. The reflectors show an abrupt pinch-out on the northern edge where a distinct moat is present, and a gradual tapering to the south. Internally we identify the base of the drift and four internal horizons, which we correlate throughout the drift. Two units display high amplitude reflectors, marked lensoidal character and restricted lateral extent, suggesting the occurrence of more energetic sedimentary conditions. Facies typical for contourite deposition are found in the sediment cores, with strongly bioturbated sediments and abundant silty/sandy mottles that contain shell fragments. These characteristics, along with the morphological and seismic information, suggest a strong control by a bottom current flowing along the moat on the northern edge of the drift. Though both Atlantic and Arctic waters are known to enter the trough, from the west and the north respectively, brine-enriched shelf water (BSW) produced during winter and flowing westward in the moat, is suggested to be responsible for the genesis of the Kveithola Drift. The formation of BSW is inferred to have started around 13 cal ka BP, the onset of drift deposition, suggesting that conditions leading to atmospheric cooling of the surface waters and/or the presence of coastal polynyas and wind or floating ice shelves have persisted on the western Barents Shelf since that time. The units inferred to have been deposited under more energetic sedimentary conditions (tentatively dated to the Younger Dryas and to 8.9–8.2 cal ka BP) are suggestive of stronger BSW formation. In general, we infer that variations in the bottom current regime were mainly related to BSW formation due to atmospheric changes. They could also have been a response to successive episodes

* Corresponding author.
E-mail address: mrebesco@ogs.trieste.it (M. Rebesco).

http://dx.doi.org/10.1016/j.quascirev.2016.02.007

of grounded and sea ice retreat that allowed for a first limited, later open shelf current, which progressively established on the western Barents Sea shelf.

1. Introduction

Sediment (or contourite) drifts are sedimentary bodies in the open ocean produced by the accumulation of sediment under the control of bottom currents (Faugères et al., 1999; Rebesco and Stow, 2001; Stow et al., 2002; Rebesco, 2005; Rebesco et al., 2008; 2014a). Bottom currents are influenced by a number of factors: foremost, on the large scale, by the global thermohaline circulation, but also by geostrophic currents, the tidal system, internal density-driven pulses and local topography (e.g. Hanebuth et al., 2015). Variations in strength and location of bottom currents are in phase with climate changes (e.g. Voelker et al., 2006). The drift deposits are generally characterized by high lateral continuity (allowing for a robust correlation of seismic profiles and cores), restricted development of hiatuses (generally of limited temporal extent), and accumulation rates higher than in the adjacent hemipelagic deposits (Rebesco et al., 2014a). These characteristics make sediment drifts an excellent repository of palaeoceanographic information.

This fact is particularly true for high latitude contourites where both bottom current strength and sediment flux are primarily controlled by extreme climatic conditions (van Weering et al., 2008; Rebesco et al., 2013). In fact, it is at high latitudes that cold, dense waters are produced, driving the global thermohaline circulation. It is also at high latitudes that sediment supply to the open ocean is dramatically enhanced at times when ice streams are grounded at or near the continental shelf edge (Laberg et al., 2012). Glacial troughs on high-latitude continental margins also contain a record of the effects of dense brine waters, produced by the formation of sea ice in polynya areas, together with supercooled water masses formed below ice shelves (Borchers et al., 2015).

Despite significant recent advances in contourite studies, a sound connection between contourite deposits, basin evolution and oceanographic processes still remains to be established (Rebesco et al., 2014a; Müller-Michaelis and Uenzelmann-Neben, 2015). In particular, there is the need to better understand the relationship between internal drift geometry and bottom current circulation, and to link the recorded sedimentary changes to variations in the paleoclimatic system.

The primary aim of this paper is to study the external and internal seismostratigraphic geometries of a high latitude sediment drift located in a glacially-carved trough in the northwestern Barents Sea, an epicontinental shelf sea of the Arctic Ocean located off the northern coasts of Norway and Russia. The drift was already briefly described by Rüther et al. (2012) and Bjarnadóttir et al. (2013) as they mainly focused their work on the glacial and deglacial history of the Kveithola Trough. On the contrary, this contribution provides unprecedentedly detailed seismic and morphological information about this sedimentary deposit, supported by some preliminary lithological and sedimentological investigation. The higher resolution of the acquired acoustic data allows for a more detailed interpretation, about the nature and characteristics of the bottom currents from which the drift was formed, providing a detailed discussion of the processes involved in the formation of the drift as well as external forcings that influenced the drift deposition and evolution. In this study, we define and correlate the main stratigraphic units that constitute the drift. On this basis, we investigate drift's evolution, i.e., the framing paleo-environmental conditions which led to the formation of these units and the sedimentary deposit as a whole. This includes a discussion of the possible bottom current flow conditions that may have controlled its growth dynamics.

2. Background

Kveithola is a glacially-carved trough located in the NW Barents Sea (Fig. 1). This trough was occupied by a fast-flowing ice stream that drained ice from Spitsbergenbanken in the north and from Bear Island in the south during the last glaciation (Andreassen et al., 2008; Rebesco et al., 2011; Rüther et al., 2012; Bjarnadóttir et al., 2013; Rebesco et al., 2014b; Llopart et al., 2015). The trough extends in E-W direction over 90 km with a width of less than 15 km and an average water depth of 300–350 m along its axis. The transverse profile of the trough is U-shaped with relatively steep flanks (dipping about 4° and locally 6° or more) and a very flat thalweg, which lies more than 150 m below the average depth of the surrounding shallow continental shelf in which it is incised. The axial profile along the thalweg is markedly staircase-like, composed of five transverse ridges about 15 km apart from each other. These ridges are composed of grounding-zone wedges (GZWs) and grounding-line fans both inferred to have formed by deposition of subglacial till and a dominance of subglacial meltwater plumes during the episodic phases of last deglacial ice stream retreat (Rebesco et al., 2011; Bjarnadóttir et al., 2013; Rebesco et al., in press). The position of GZWs was likely controlled by small pre-existing morphological steps generated by NNW-SSE faults and/or wave-cut terraces (Lebesbye and Vorren, 1996). These normal faults (the easternmost and major one being the Knølegga Fault at the eastern termination of the Kveithola Trough) belong to a faulted basin geometry that for most parts reflects phases of extension associated with the opening of the Norwegian - Greenland Sea since the Cretaceous (Gabrielsen et al., 1990; Bergh and Grogan, 2003). We infer that these faults also generated the structural depressions ("channels"), which we observe to the north and south of the inner part of the Kveithola Trough (Fig. 1). Apart from the structural control, the present-day seafloor morphology is largely inherited from the paleo-seafloor topography which formed at the time of GZW formation. Following deglaciation, this morphology was draped by a relatively uniform glaciomarine blanket more than 15 m thick. This glaciomarine blanket covers the whole trough and is inferred to be characterized by plumites and ice-rafted debris (Rebesco et al., 2011; Bjarnadóttir et al., 2013; Lucchi et al., 2013; Hanebuth et al., 2014; Llopart et al., 2015). Finally, a sediment drift (the "Kveithola Drift") is present in the inner part of the trough associated to a field of pockmarks (Bjarnadóttir et al., 2013). This drift is inferred to have been formed by sediments supplied by dense bottom currents, mainly infiltrating via a large channel that is connected to the innermost Kveithola Trough from the north (Thomsen et al., 2001; Bjarnadóttir et al., 2013). While Bjarnadóttir et al. (2013) gave a general account of glacial, deglacial to Holocene acoustic units of the Kveithola Trough, this manuscript focus on the Holocene Kveithola drift units described in far greater detail. The PARASOUND, operated at 4 kHz, provides a much higher resolution than the Chirp data presented in Bjarnadóttir et al. (2013) and Rüther et al. (2012). The drift deposit that was initially subdivided

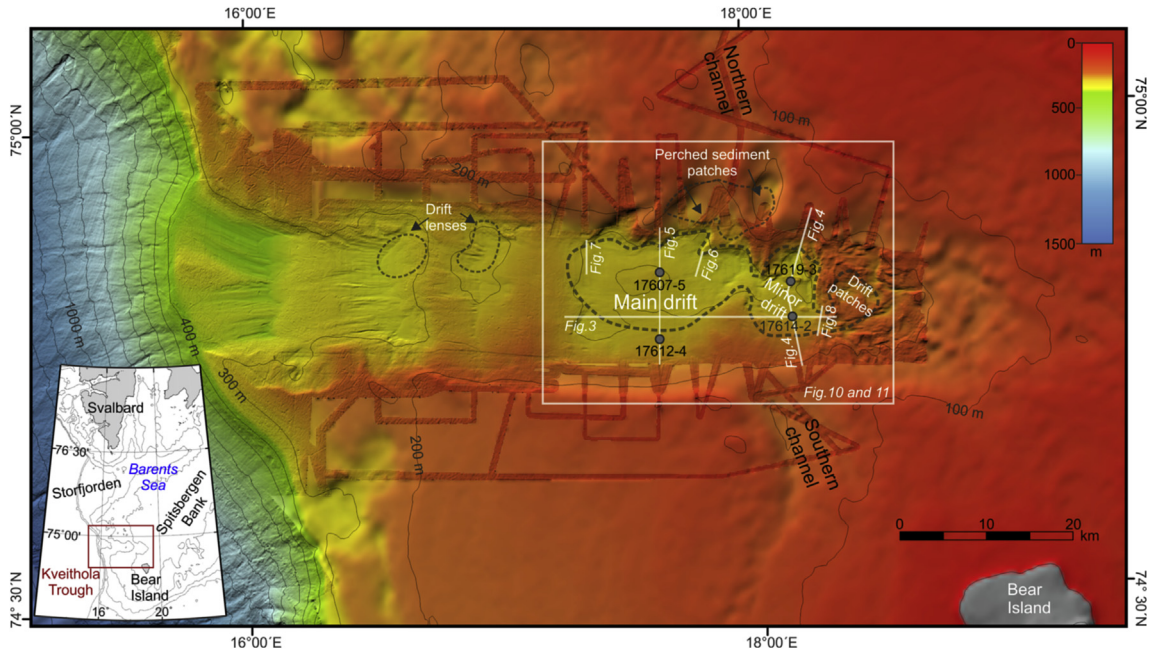

Fig. 1. Bathymetric map of the Kveithola Trough produced using all available multibeam datasets (see text for details) superimposed onto IBCAO data (Jakobsson et al., 2012). Grid size: 20 m for depth less than −700 m depth and 40 m for deeper data; vertical exaggeration: 2.7; Light Direction Attitude 35°; Azimuth −30°. The location of the PARASOUND sediment echosounder profiles and of sediment coring sites presented in this paper are indicated, and the box shows the location of Fig. 10. A dashed black line indicates the outline of the Kveithola drift bodies. Location map of the study area is shown in the bottom-left corner.

in two subunits (CU1 and CU2) by the latter authors, is now subdivided in five units thanks to the detailed PARASOUND record. The Drift chronology previously suggested by Rüther et al., 2012 is strengthened by the new dates presented in this paper.

The Kveithola drift complex developed after the Last Glacial Maximum (LGM) that took place at about 21.5 cal ka BP (calibrated thousands-years before present) when the ice reached the shelf break at the western Barents Sea margin (Vorren and Laberg, 1996). According to Bjarnadóttir et al. (2013), the onset of deglaciation in the Kveithola Trough may have coincided with that of the larger Storfjorden paleo-ice stream trough located south of Svalbard (Pedrosa et al., 2011; Camerlenghi et al., in press) at about 20–19 cal ka ago (Rasmussen et al., 2007; Jessen et al., 2010; Lucchi et al., 2013, 2015). However, it took several thousands of years before the Kveithola Trough was completely free of ice. In fact, the upper part of the glaciomarine blanket was deposited during the Late Bølling/Allerød interval (about 14.2–13.9 cal ka BP according to Rüther et al., 2012), and the lower part of the blanket is inferred to have started to deposit at the beginning of the Bølling interstadial (Rüther et al., 2012; Bjarnadóttir et al., 2013) which coincides with the start of the global Meltwater Pulse 1a (14.65 cal ka BP, Deschamps et al., 2012). According to Rüther et al. (2012), the Kveithola sediment drift was deposited after 13.1 cal ka BP. For the upper part of the drift, an age of about 11.2–10.3 cal ka BP is inferred by Rüther et al. (2012), who also identified a sand unit deposited after about 8.2 cal ka BP, coinciding with the 8.2 ka climate event (Alley et al., 1997) and the associated meltwater pulse event MWP-1c (Blanchon et al., 2002; Bird et al., 2010). The drift thins out at the coring sites studied by Rüther et al. (2012) who sampled the drift only in its peripheral area, where the thickness is one tenth of that recorded in the depocenter. Therefore, only the lower part of the drift (Drift 2 of Bjarnadóttir et al., 2013) was sampled and studied by Rüther et al. (2012). As the previously studied cores are not from the thick part of Drift 2, it is uncertain whether they can contain the youngest part of Drift 2 sediments. It is equally dubious if any of the sediments forming the upper part of the drift (Drift 1 of Bjarnadóttir et al., 2013) was present in the cores studied by Rüther et al. (2012). It was, however, believed by these authors that at least a thin interval of Drift 1 sedimentary sequence was present in their cores, inferred to be of early Holocene age.

Palaeoecological and palaeoceanographic changes in the nearby brine-enriched environment of the Storfjorden Trough occurred in relation to past climate changes since LGM have been recently constrained through the distribution of benthic calcareous and agglutinated foraminiferal species (Rasmussen and Thomsen, 2014, 2015). The outer shelf of Storfjorden Trough experienced open marine conditions during the deglaciation from about 15 to 11.7 ka BP, whereas the inner part was still occupied by grounded ice. The study by Rasmussen and Thomsen (2014, 2015) revealed that enhanced sea ice and stronger brine formation occurred during the cold periods including the Older Dryas, the Intra-Allerød Cold Period and the Younger Dryas. In general, the colder periods show a stronger influence of Arctic water, with higher brine production and more corrosive bottom water, whereas warmer periods show a stronger influence of Atlantic Water and decreased influence of brine production.

3. Hydrographic setting

The western margin of the Barents Sea is influenced by the West Spitsbergen Current (Fig. 2), a warm and saline Atlantic-derived water that flows northwards along the eastern side of the Fram Strait (e.g. Aagaard et al., 1973; 1987). Some branches of this current enter the Barents Sea (e.g. Poulain et al., 1996). Recent studies have documented the ability of this current to transport sand-sized sediments and to generate sand waves in the outer Bear Island Trough (King et al., 2014; Bøe et al., 2015). The bottom circulation pattern is strongly influenced by the topography so branches from the main current penetrates into the glacial troughs on the continental shelf (e.g. Storfjorden, Bjørnøyrenna, and possibly Kveithola

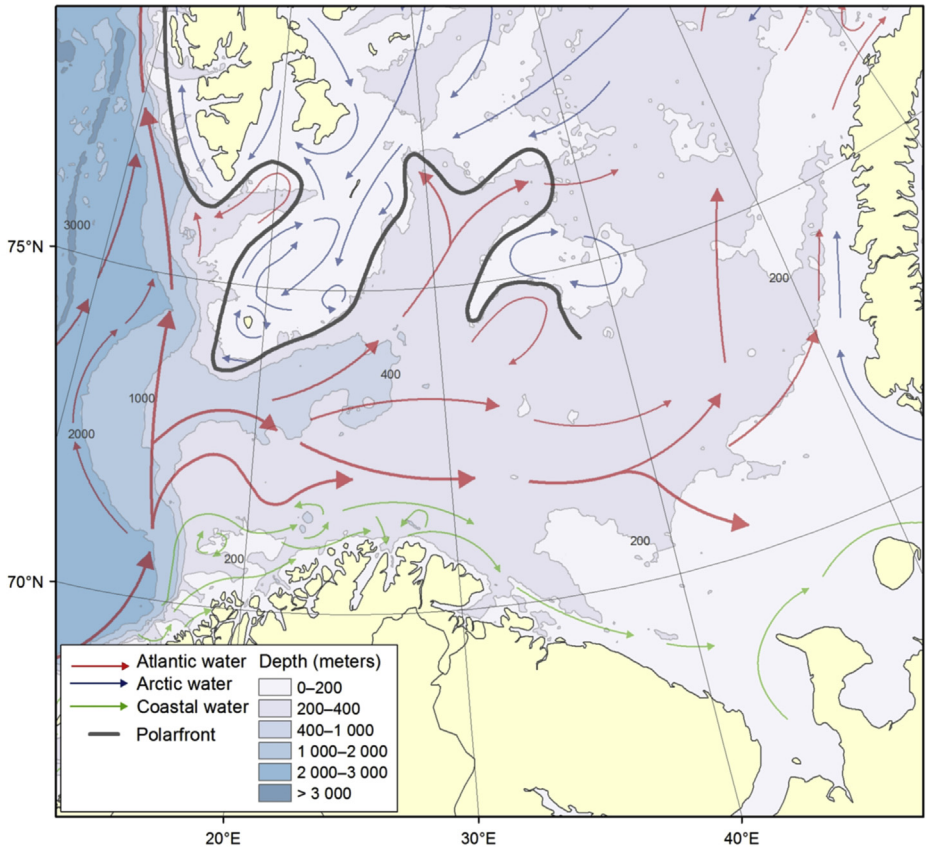

Fig. 2. The main features of the circulation and bathymetry of the Barents Sea. Modified after Stiansen and Filin, 2007. Courtesy of Karen Gjertsen, Norwegian Institute of Marine Research. To be noticed the branches of the West Spitsbergen Current penetrating into the glacial troughs on the continental shelf (e.g. Storfjorden, Bjørnøyrenna, and possibly Kveithola Trough), following the contours and eventually turning and exiting again toward the continental slope.

Trough), following the contours. When the bottom current encounters a topographic barrier, it turns laterally and backwards toward the continental slope (e.g. Midttun, 1990; Fohrmann et al., 2001; Stiansen and Filin, 2007) after being efficiently mixed and cooled down on the shelf. In fact, the Atlantic Water in the Barents Sea is cooled by the atmosphere and mixing occurs through wind, wave, and ice motion, leading to the formation of the Arctic Surface Water (Boyd and D'Asaro, 1994). In the northern part of the Barents Sea fresh and cold Arctic Surface Water flows from northeast to southwest (Fig. 2) reaching Spitsbergenbanken and the Kveithola Trough (Midttun, 1990; Stiansen and Filin, 2007).

Dense bottom-water masses are produced on the Barents shelf during winter (Aagaard et al., 1985; Thomsen et al., 2001) as a consequence of atmospheric cooling, as well as sea-ice freezing and brine rejection (Rudels and Quadfasel, 1991). Summer remnants of brine-enriched shelf water (BSW) in morphological shelf depressions have been observed in several areas of the Barents Sea (Quadfasel et al., 1988; Blindheim, 1989). The BSW collected in such depressions flows to the shelf edge in the form of gravity plumes and cascades down the continental slope (Aagaard et al., 1985; Quadfasel et al., 1988; Jungclaus et al., 1995; Schauer, 1995). Kveithola in particular, connected to a system of structurally-controlled channels that drain parts of the Spitsbergen and Bear Island Banks, operates as a drainage system for BSW (Fohrmann et al., 1998, and references therein; Thomsen et al., 2001). The source water of the observed outflow is provided by the East Spitsbergen Current, advecting Arctic Water during summer and early winter, and a mixture of Arctic and Atlantic Waters during late winter (Schauer, 1995). On its way, the BSW flow is assumed to erode the seafloor and transport sediment into the deep sea, resulting in cascading of high-density turbidity plumes that may contribute to maintain the gullies free of sediment still today (Fohrmann et al., 1998; Llopart et al., 2015). Such turbidity plumes, mainly active during deglaciation, result in a high-accumulation area on the Storfjorden Trough-Mouth Fan (Fohrmann et al., 2001). In fact, several intrusions of turbid water up to 200 m thick were observed at and simulated for the upper continental slope (Fohrmann et al., 1998), strongly correlating with temperature and salinity inversions, which indicate advection of shelf bottom water from the Kveithola Trough (Thomsen et al., 2001).

4. Materials & methods

Multibeam bathymetric data were acquired during four different cruises with different vessels: SVAIS (Camerlenghi et al., 2007), EGLACOM (Zgur et al., 2008), GlaciBar (Andreassen et al., 2009), and CORIBAR (Hanebuth et al., 2013). The four datasets have been jointly reprocessed at OGS by importing all data in Caris Hips&Sips. Refraction problems were likely generated by closely spaced velocity changes in the water column, not always adequately sampled by the acquired SVP probes. We corrected for refraction problems during post processing with the refraction tool at our disposal in Caris. We applied Admiralty TablesTide on all datasets. To reject spurious data we used a surface filter based on 2D editing in Subset Editor. Caris Fieldsheets were exported in xyz and imported in Global Mapper UTM 33 WGS84 (20 m grid size for depth less than −700 m and 40 m for deeper data). To maximize seafloor morphology we used a vertical exaggeration of 2.7 and

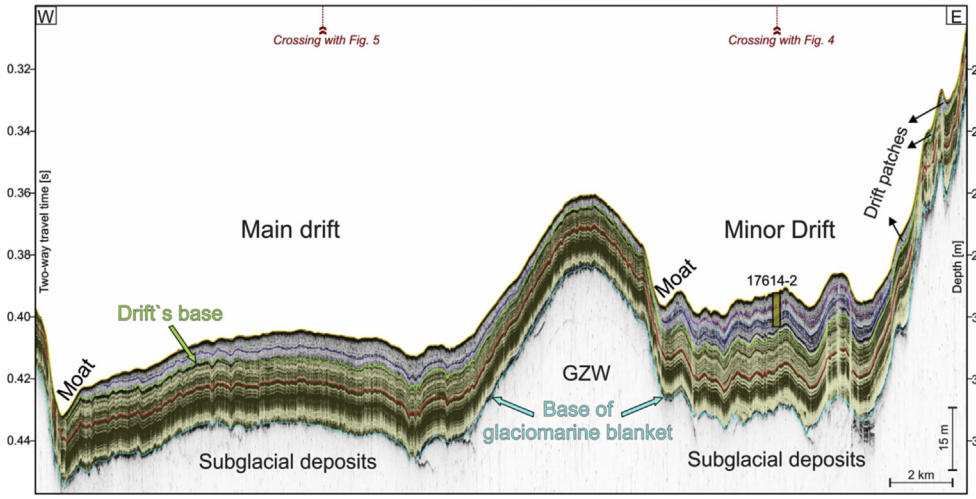

Fig. 3. Longitudinal E-W trending PARASOUND profile across the main and minor Kveithola Drift body. The morphology of the drift is strongly controlled by the morphology of the underlying stratigraphic units. The drift thins across a pre-existing bathymetric high (a GZW), whereas the underlying glaciomarine blanket (highlighted in yellow in all seismic profiles) is less affected (almost constant thickness). See location in Fig. 1. (For interpretation of the references to colour in this figure legend, the reader is referred to the web version of this article).

Light Direction Attitude 35°, Azimuth −30°. We imported IBCAO 73–78°N (UTM33), created an opportune common colorscale, and a contour layer based on all used dataset layers.

Parametric sediment echosounder data used in this study were acquired using the shipboard hull-mounted PARASOUND system (Atlas Hydrographic) on board of the German R/V Maria S. Merian during the MSM30 (CORIBAR) cruise in 2013 (Hanebuth et al., 2013). The Kveithola Trough and its drift deposits (including the perched sediment patches infilling a 50-km long, structurally controlled shallow-shelf channel connected to the inner trough from north) were covered with a dense grid of PARASOUND profiles. The chosen frequency of 4 kHz provides a vertical resolution of up to 20 cm, whereas the horizontal resolution is approximately 7% of the water depth. The maximum penetration of the acoustic signal was close to 40 m (estimated using a sound velocity of 1500 m/s for depth conversion). The PARASOUND data were processed and converted to seg-y data format using in-house developed software (H. Keil, University of Bremen), and successively displayed with the Kingdom Suite software (Seismic Micro-Technology).

A Gravity Corer with the variable lengths of 3, 6, or 12 m and a top weight of 1.5 tons was deployed within the Kveithola Trough during the CORIBAR cruise at 11 stations, and selected examples from these sediment cores are presented in this paper (see Table 1). Two cores (GeoB17607-5 and GeoB17612-4) were collected on the main drift body and two (GeoB17619-3 and GeoB17614-2) on the minor drift body. Of these, two (GeoB17607-5 and GeoB17619-3) are located on the center of the drift that is thick and well stratified, and two (GeoB17612-4 and GeoB17614-2) are located on southern flank of the drift where the PARASOUND data show a condensed succession. Before the cores were split for visual description and sampling, they were scanned with the Multi-Sensor Core Logger (MSCL) at MARUM (University of Bremen, Germany) using a step size of 1 cm for gamma-ray density and magnetic susceptibility measurements.

Five dating points (Table 2) were opportunely taken from the end of the core sections, before splitting (Grave, 2014). Those samples were collected in order to have a preliminary reference information about the ages of the drift. Suitable samples of in-situ preserved bivalve shells, and scaphopods, were carefully selected for radiocarbon dating and measured at the accelerator mass spectrometer (AMS)-^{14}C Radiocarbon Laboratory Poznan, Poland. The results were calibrated with CALIB v. 7.1.0 (Stuiver and Reimer, 1993) using the Marine13 calibration data set (Reimer et al., 2013) with an average marine reservoir effect dR = 67 ± 34 for the area south of Spitsbergen (Mangerud and Guliksen, 1975). The mean values from the calibrated age range of ±1sigma are normalized to calendar year and indicated as *cal a* BP (or *cal ka BP*). In addition, the Median Probability (MP) of the probability distribution that is determined by the software, is reported as more reliable estimation of the sample calendar age (Telford et al., 2004; online Calib Manual).

5. Results

5.1. External geometry of the drift

The Kveithola sediment drift has a complex morphology, comprising a main, outer drift body, about 200 km^2 in extent, and a minor, inner one about 100 km^2. In addition there are several small depocenters associated to these two deposits: two drift lenses as already highlighted by Bjarnadóttir et al. (2013) in the outer part of the Kveithola Trough (about 20 km^2), more or less connected patches of local drift deposits in the innermost part of the Kveithola Trough, and other small perched sediment patches in local depressions in the channel north of the trough (Fig. 1). The existence of further patch drifts in local depressions outside Kveithola Trough, beyond the coverage of our sub-bottom data, cannot be excluded.

The drift, comprised of lensoidal units, shows a thickness of up to over 30 ms in its center and thins towards the margins (Fig. 3). These units rest on top of a sub-parallel, more laterally continuous blanket. Overall, the drift has a broadly mounded shape. However, the geometry of the drift is largely controlled by the morphology of the underlying stratigraphic units. In fact, the highs within the drift correspond to elevated areas of the underlying glacial units. The disconnection of the main (outer) and minor (inner) drift body is similarly related to the underlying morphology: a buried GZW, transverse to the axis of the Kveithola Trough, is located between the main and minor drift bodies, and only covered by a greatly reduced drift thickness (less than 5 ms). Due to this topographic control by the underlying strata, the morphology of the drift is

Table 1
Sediment cores.

Core ID	Core location	Coordinates	Water depth (m)	Sediment recovery (cm)
GeoB17607-5	Center of the main drift	74°50.71′ N 17°38.28′ W	298	920
GeoB17612-4	Southern flank of the main drift	74°46.46′ N 17°37.75′ W	287	270
GeoB17614-2	Southern flank of the minor drift	74°47.64′ N 18°08.76′ W	287	796
GeoB17619-3	Center of the minor drift	74°49.64′ N 18°09.28′ W	298	682

Table 2
Radiocarbon dating.

Core ID	Lab ID	Depth bsf (cm)	Sample type	^{14}C age (cal a BP)	1σ range (cal a BP)	2σ range (cal a BP)	Median probability (cal a BP)
GeoB17607-5	Poz-63467	920	Scaphopods	9250 ± 50	9891–10,107	9754–10,160	9980
GeoB17612-4	Poz-64368	185	Bivalve shell	10,230 ± 50	11,106–11,2222	11,010–11,2900	11,160
GeoB17612-4	Poz-64369	270	Planktonic foraminifera	11,200 ± 50	12,591–12,6933	12,547–12,7577	12,650
GeoB17614-2	Poz-64371	Core catcher	Bivalve shell fragments	11,600 ± 50	12,929–13,1011	12,820–13,1722	13,010
GeoB17619-3	Poz-64372	498	Scaphopods	8330 ± 40	8713–8919	8624–8970	8800

complex, showing several local highs, and the areas of maximum thickness (highest sedimentation rate) do not necessarily correspond to bathymetric highs or basement lows (see Fig. 3).

The thinning by lateral termination of the internal seismic reflectors occurs in an asymmetric way with an abrupt pinch-out on the northern edge and gradual tapering on the southern edge (Figs. 4 and 5). To the south the drift has a sedimentary tail that progressively thins southward due to reduced sedimentation rate during deposition as shown by the seismic profiles (see the following chapter). This tail onlaps the southern flank of the Kveithola Trough and its tip is located at about 250 m water depth, thus about 50 m shallower than the central, mounded part of the drift found at about 300 m water depth.

5.2. Internal geometry of the drift

The seismic expression of the Kveithola Drift is mainly well-stratified, characterized by sub-parallel reflections of moderate to high amplitude and good lateral continuity, without any major unconformity. The subdivision of the sedimentary fill into seismic units was done by means of an analysis of reflection terminations and internal reflector patterns (Fig. 6). In the following, we describe reflection horizons and intervening seismic units stratigraphically from bottom to top:

5.2.1. Horizon 1 (cyan)

Bottom of the glaciomarine unit and top of the underlying glacial till. The horizon is identifiable throughout the whole trough, marking the change from transparent (below) to layered (above) strata and is concordant with the overlying Horizon 2.

5.2.2. Unit 1.a

Reflections with the highest amplitudes are observed within this unit. However, they become faint and semi-transparent

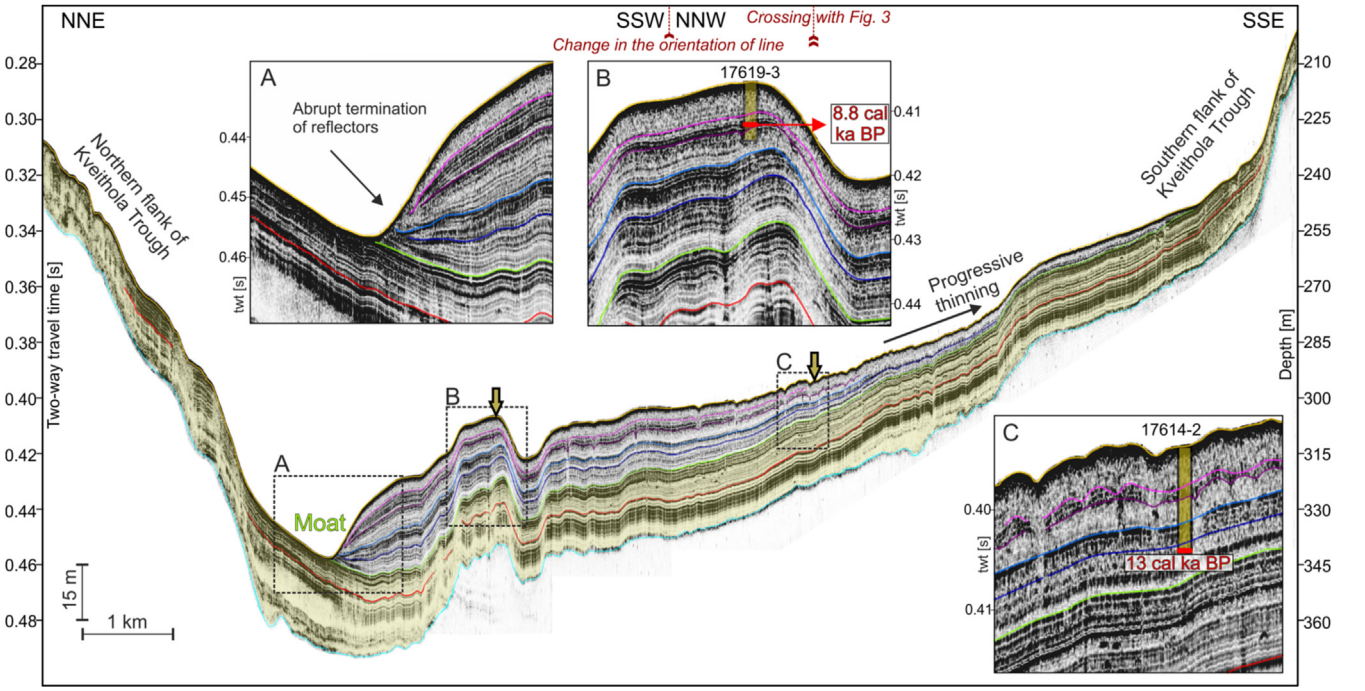

Fig. 4. Transversal NNE-SSW PARASOUND profile across the main Kveithola Drift body. The drift shows an abrupt pinch out towards the moat on the northern edge and a progressively thinning tail on the southern edge. Locations of core GeoB17607-5 from the central (expanded) part of the drift and of core GeoB17614-2 from the marginal (condensed) part of the drift are also shown. See location in Fig. 1.

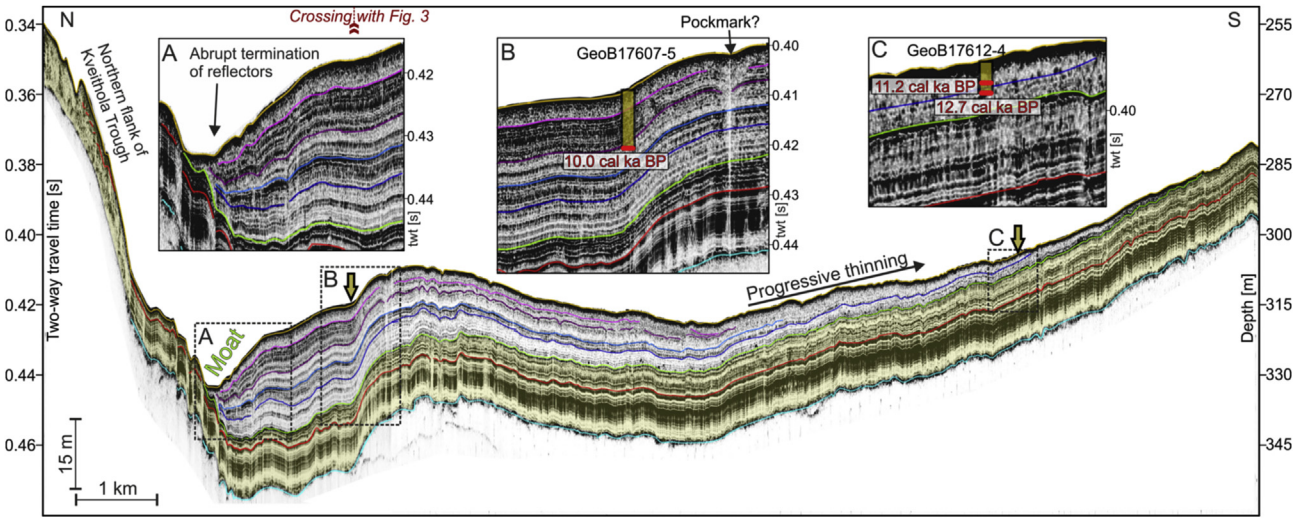

Fig. 5. Transversal N-S PARASOUND profile across the main Kveithola Drift body. Locations of core GeoB17619-3 from the central (expanded) part of the drift and of core GeoB17612-4 from the marginal (condensed) part of the drift are also shown. See location in Fig. 1.

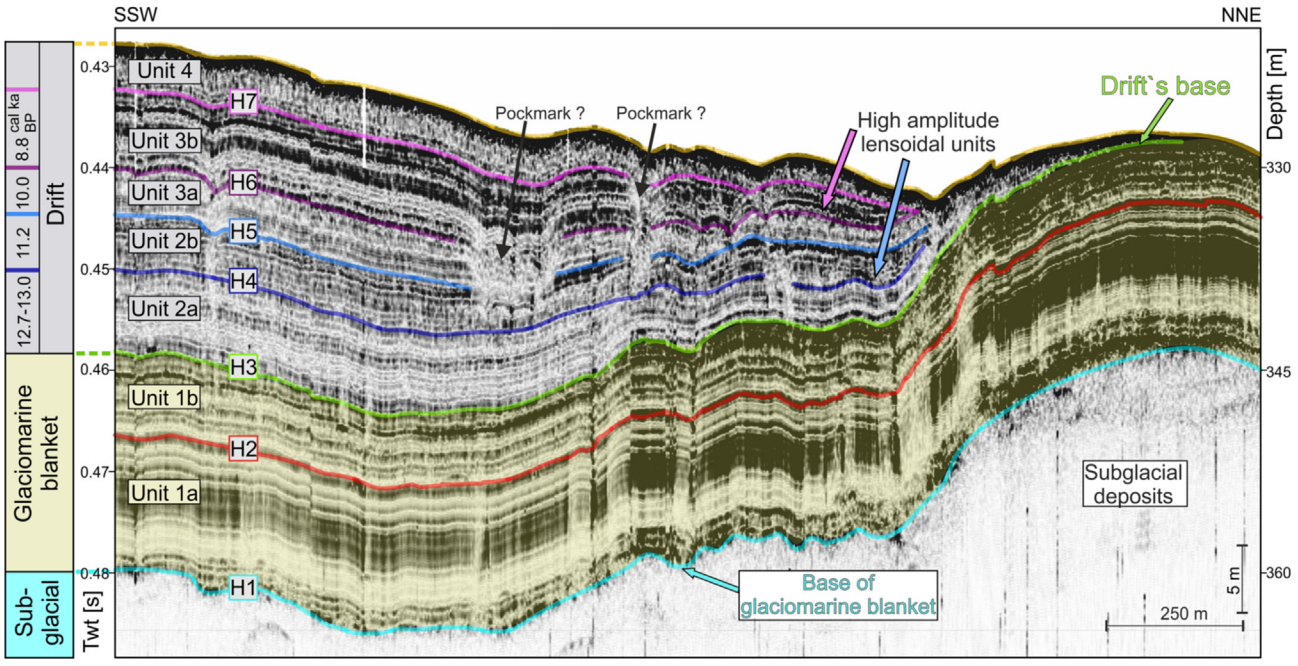

Fig. 6. Close up of NNE-SSW PARASOUND profile across the northern edge of the Kveithola Drift. Identified seismic horizons and intervening units are indicated. The available datings are indicated in the column to the left. The relatively minor extent and higher amplitude of Units 2.b and 3.b are apparent. See location in Fig. 1.

towards the bottom and top of this unit. Reflector configuration within the unit is parallel. The thickness of this blanket unit (about 15 ms) is laterally remarkably uniform. Although reflections are continuous and parallel inside the trough, this continuity is often lost at the flanks.

5.2.3. Horizon 2 (red)

Main internal acoustic boundary of the glaciomarine blanket. This distinct regional reflector corresponds to reflector D1 of Rebesco et al. (2011).

5.2.4. Unit 1.b

This unit is made of moderate amplitude, high-frequency, parallel internal reflections. The lower part of this unit is the upper section of the glacigenic blanket.

5.2.5. Horizon 3 (green)

Base of the drift, which overlies concordantly Unit 1.b. This horizon marks a sharp change in acoustic facies from the well-layered, moderate-amplitude reflections of the unit 1.b to lower amplitudes above. It corresponds to the base of drift 2 of Bjarnadóttir et al., 2013 (see Table 3).

5.2.6. Unit 2.a

This unit has low amplitude reflectors. The basal reflections terminate in an onlap onto Unit 1.b at the periphery of the drift. In some cases a sedimentary mound with downlap in both directions is observed (Fig. 7).

Table 3
Comparison, using two crossing sub-bottom profiles, between the seismostratigraphic interpretation of this study (profile 20130724-014159) and that of Bjarnadóttir et al., 2013 (profile 09KA_JM081). In the two outermost columns the available datings (in cal. ka BP) are indicated.

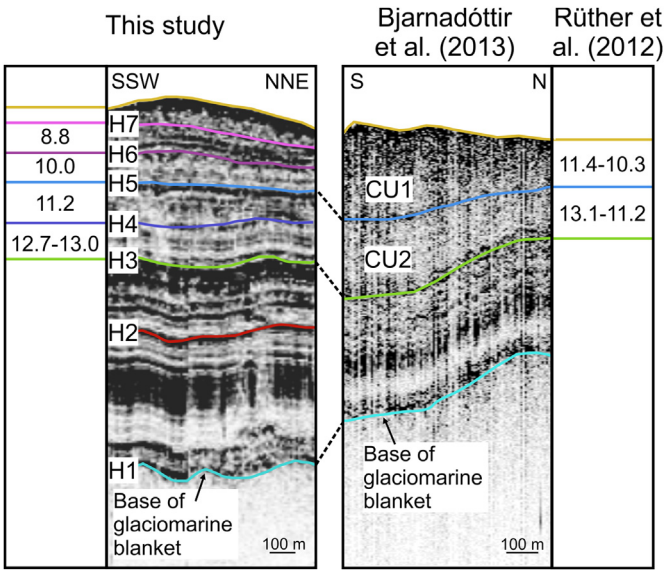

5.2.7. Horizon 4 (dark blue)

Strong internal reflector within the lower part of the drift. It marks the change from low amplitude reflectors (below) to moderate amplitude reflectors (above).

5.2.8. Unit 2.b

The amplitude of reflectors in this unit is generally higher than in the underlying one and increases upward in many cases (Fig. 6). Local downlap onto the underlying Horizon 4 is often noticeable (Fig. 7).

5.2.9. Horizon 5 (light blue)

Top of the lower part of the drift (top of drift 2 of Bjarnadóttir et al., 2013). Locally, the continuity of this boundary is interrupted by small depressions (interpreted as paleo-pockmarks).

5.2.10. Unit 3.a

Semi-transparent unit at the base of the upper part of the drift (the drift 1 of Bjarnadóttir et al., 2013).

5.2.11. Horizon 6 (dark pink)

Local, small-scale depressions or paleo-pockmarks are present along this boundary (Fig. 6). It marks the change from low amplitude reflectors (below) to moderate amplitude reflectors (above).

5.2.12. Unit 3.b

This unit has relatively high amplitude reflectors, which is generally increasing towards the top (Fig. 6). Local downlap onto the underlying Horizon 6 is often noticeable.

5.2.13. Horizon 7 (pink)

This reflector marks the transition from relatively high

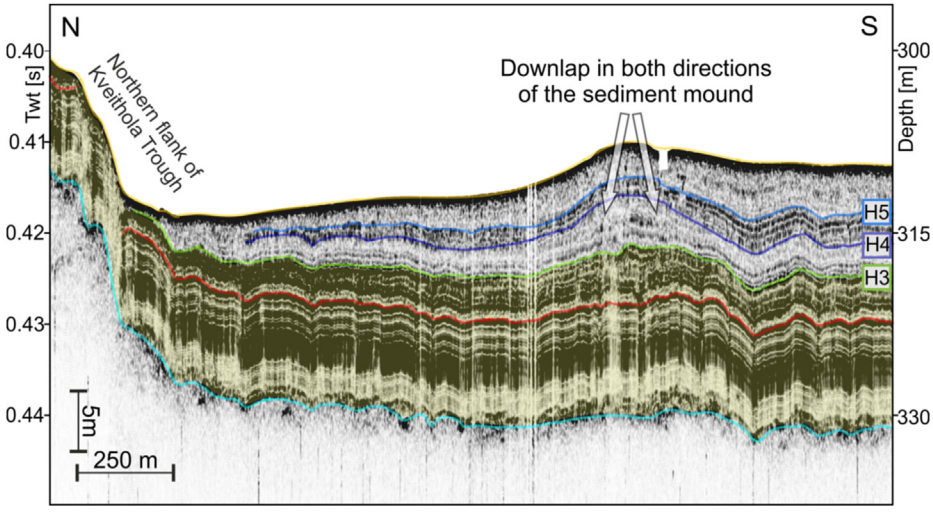

Fig. 7. Close up of N-S PARASOUND profile across a mounded feature on the western edge of the Kveithola Drift. A marked downlap in both directions can be observed within this small sedimentary mound. See location in Fig. 1.

amplitude reflectors (below) to very low amplitudes (above).

5.2.14. Unit 4

This unit is has very low amplitude reflectors and it appears, in pseudo-relief plots, to be almost acoustically transparent

5.2.15. Seafloor (yellow)

The seafloor is always a very high amplitude reflector, locally showing small depressions interpreted as pockmarks (e.g. Figs. 5b and 6).

The depocenter onlaps onto the underlying well-stratified units at its periphery and onto the underlying highs (GZW). The reflection amplitudes tend to vary vertically in a recurrent pattern (Figs. 4–6). In particular, two units display high amplitude reflectors (Units 2.b, 3.b). These units show a lensoidal character (mainly towards the periphery of the drift) and are of restricted lateral extension. In fact, their margins terminate in advance with respect to the underlying and overlying more transparent units (Fig. 6).

Nonetheless, the most distinctive feature of the drift is the termination of reflectors towards the moat, i.e., the channel-like morphological depression along its northern edge (Figs. 4–5). This termination, locally very abrupt with a reduction of more than 20 m in thickness over a distance of only a few hundreds of meters, seems to be produced initially by erosion and later by persistent non-deposition (Figs. 4–5). In fact, the moat is mainly produced by downlap and pinching out of drift strata against the top of the underlying glaciomarine blanket that drape the entire Kveithola Trough. Close to the termination, the lower reflectors of the drift dip towards the center of the Kveithola Trough like those of the glaciomarine blanket, but the upper reflectors of the drift dip into opposite direction due to the progressive thickening at the center of the drift, which continued to the present (see the close-up A in Fig. 4). In general, the lower drift units (Units 2.a and 2.b) close to the moat are more affected by erosion, whereas the upper drift units (Units 3.a and 3.b) are more affected by downlap termination. Downlap is also visible at the base of the drift (onto the green Horizon 3) within local sediment mounds (Fig. 7).

The internal character of the drift body located at the innermost part of the Kveithola Trough is condensed and it is not possible to distinguish different internal units (Fig. 8). In that area the drift is constituted of transparent facies and seems to present several adjacent depocenters or connected patch-drifts.

5.3. Lithological characteristics and sedimentary sequence

The sedimentary sequence recovered in the area of the Kveithola drifts contains two main stratigraphic intervals. The younger one is formed by heavily bioturbated sediments with abundant silty/sandy mottles, and sparse shell fragments (light and dark cyan backgrounds in Fig. 9). The older stratigraphic interval is characterized by higher values of magnetic susceptibility and lower values of wet bulk density (light and dark pink backgrounds in Fig. 9). Articulated bivalve shells and scaphopod tubes, both in life position, occur scattered throughout the sediment and were the most suitable targets for dating (Fig. 9). The sediments are bioturbated and locally finely laminated (e.g. core 17612-4, 2.55–2.70 m; 17614-2, 4.20–6.60 m). Sparse IRD occur at the base of core 17614-2. The transition between the two main stratigraphic intervals corresponds to an irregular, possibly erosive surface, that is overlain by normally graded sediments located at the base of the younger interval as detected during the visual description of the cores. In core 17612-4, the graded sands at the base of the younger interval, contain mud chips (Fig. 9), whereas in core 17607-5 such transition appear more gradual. According to our radiocarbon dating the transition between the two stratigraphic intervals occurs at 8.8 cal ka BP (based on core 17619-3, Table 2).

Core correlation based on the lithological succession, magnetic susceptibility and the five radiocarbon dates (Table 2), reveals that core 17607-5, located in the center of the well-stratified main, outer drift body, contains the most expanded (high-resolution) sequence, recording the last 10 ka; core 17619-3, located in the center of the minor, inner drift body (eastern part, Fig. 1), contains a more condensed succession; and cores 17614-2 and 17612-4 located along the southern flank of the minor and main drift bodies, respectively, recovered the most condensed part of the drift depocentre spanning the last 13 ka.

6. Interpretation

We consider the abrupt termination to the north of the internal reflectors of seismic Units 2a to 4 and the broadly mounded geometry of the Kveithola Drift as principal diagnostic features allowing it to be interpreted as a bottom current-controlled sediment drift. This interpretation is consistent with the sediment characteristics observed in the core dataset (see Stow and Faugères, 2008 and references therein for contourite facies) and with the interpretation of Bjarnadóttir et al. (2013), who first recognized the presence of a drift within the Kveithola Trough. Furthermore, we interpret that the moat, with reflector termination along the northern edge of the drift, to have been formed by focused bottom currents (Faugères et al., 1999; Rebesco and Stow, 2001; Stow et al., 2002; Rebesco, 2005; Rebesco et al., 2008; 2014a). This moat extends as a laterally continuous feature along the entire northern

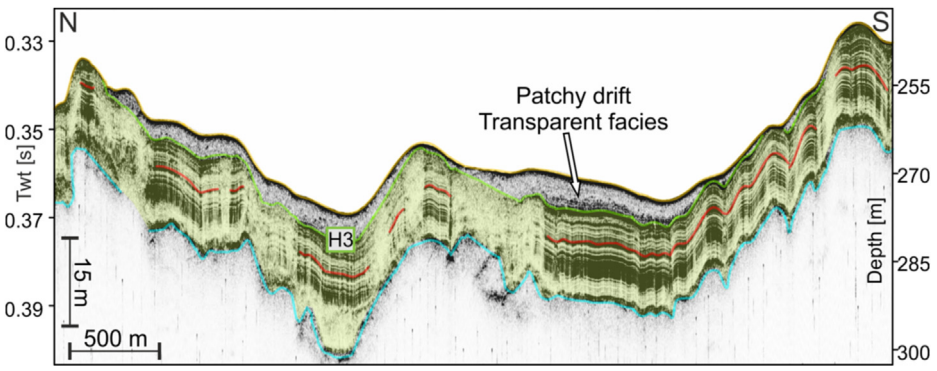

Fig. 8. Transversal N-S PARASOUND profile across the western edge of the innermost part of the Kveithola Drift. In this area the drift shows a condensed, transparent facies and includes several depocenters or connected patch-drifts. See location in Fig. 1.

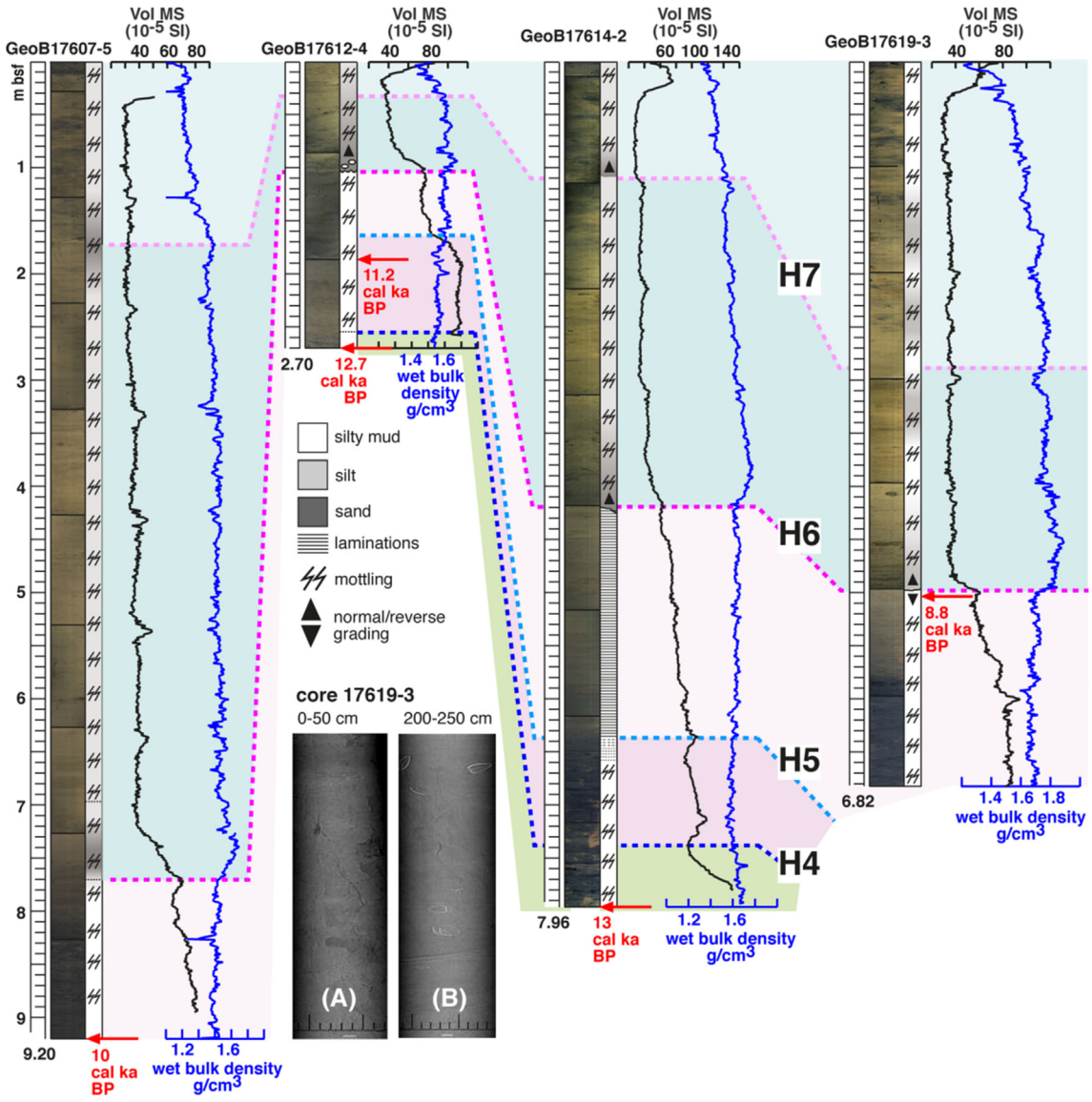

Fig. 9. Down core logs of four selected cores from the main and minor Kveithola Drift bodies showing sediment photographs, lithology (log), magnetic susceptibility (black curve) and bulk density (blue curve). Core correlation is based on sediment facies, magnetic susceptibility and wet bulk density trends, and 5 calibrated 14C dates (red arrows). Two x-ray facies are also included to show two typical sedimentary structures: bioturbated mud (A) and articulated bivalve shells (B). Core location in Fig. 1. (For interpretation of the references to colour in this figure legend, the reader is referred to the web version of this article).

edge of the drift, with local bends and a more pronounced character in correspondence of local morphologic promontories. The moat therefore provides a means to reconstruct the path of the inferred bottom current flow that controlled the development of the sediment drift and its geometry (Fig. 10).

Conversely, no moat is visible on the southern edge of the drift. In some places a polished floor with relatively coarser sediments (swept by bottom currents) borders the southern margin of the drift where the slope locally steepens. Nonetheless, the drift sediments are thinning very gradually to the south, and eventually terminating at a seafloor depth much shallower than that of the moat on the northern edge (Figs. 4 and 5). The drift is hence confined to the deeper part of the Kveithola Trough, but it does not display the typical geometry of confined drifts. Such drifts are typically mounded, elongated along the main axis of the trough and show a moat on both flanks of the trough (Faugères et al., 1999; Stow et al., 2002; Rebesco et al., 2014a). In the typical confined drift case, the bottom current flows in opposite directions on the two opposing flanks of the drift. The hypothesis of a confined drift is, however, not completely discarded for the Kveithola Drift, but the typical confined drift case described in the literature does not seem to apply here. This may be due to the fact that the bottom current flows on one flank of the drift differs significantly from that on the opposite side (see the following discussion in the chapter "Water masses responsible for drift genesis").

It is often a challenge to differentiate whether a stratified, slope-related depocenter is mainly built up by current-controlled (contouritic) or by gravity-driven (turbiditic) sedimentation processes (Rebesco et al., 2014a). Thus, the diagnostic information obtained needs to be interpreted carefully. A turbiditic system would result in a uniform or fan-like infill of pre-existing depressions with ponding of reflectors in the deepest parts and onlap at the depression margins. The geometry of the Kveithola drift (Figs. 4 and 5) show downlaps and a moat, suggesting that some contribution

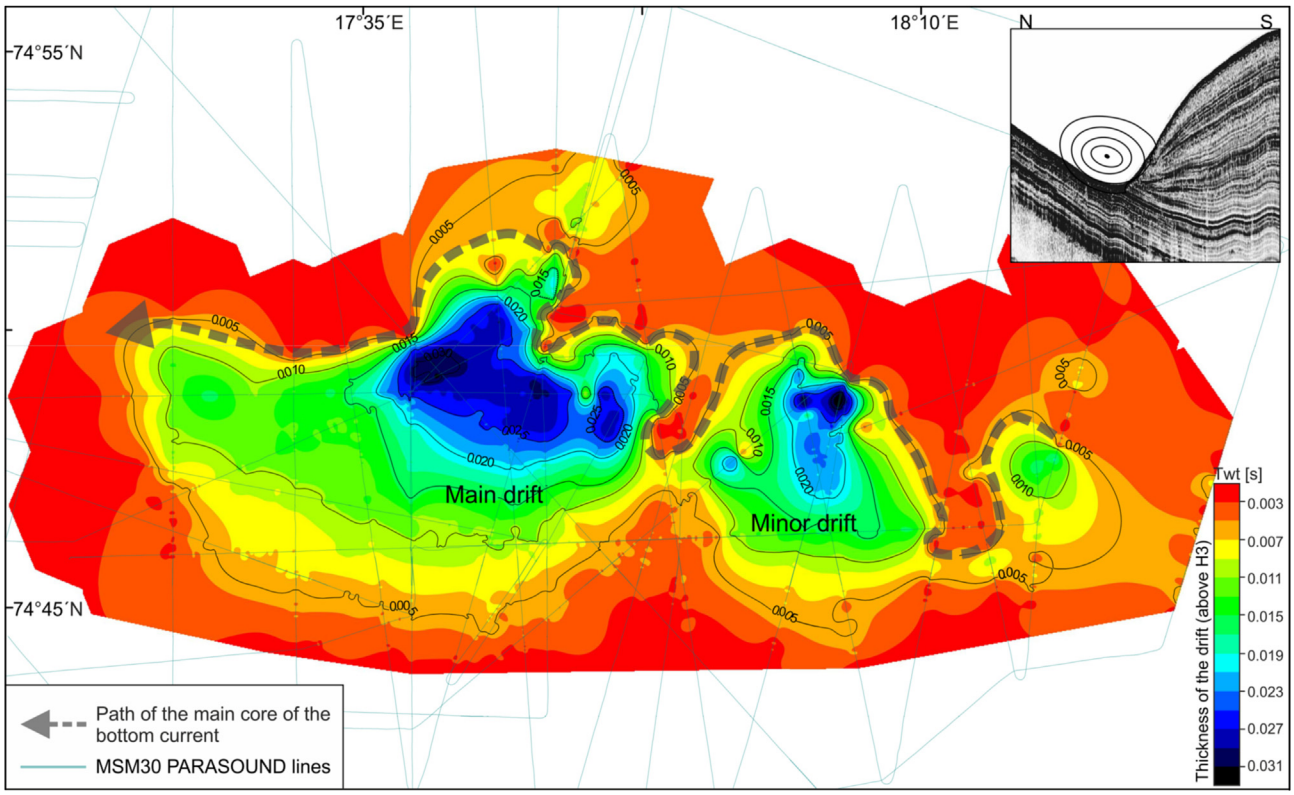

Fig. 10. Isochore time map showing the sediment thickness (in seconds) of the Kveithola Drift. Location of all PARASOUND profiles acquired in the drift area during cruise MSM 30 is also shown. The detailed path of the main core of the bottom current (dashed line) is interpreted by connecting the position of the moat in the various PARASOUND profiles. The inset shows an example of the moat visible in seismic section with drawing of the inferred core of the bottom current.

of sediments from turbidity currents to the formation of the sedimentary body occurred (e.g. irregular surfaces overlay by normally graded sands with mud chips of core 17612-4, Fig. 9) but it was completely subordinate, at a large scale, to bottom water reworking of sediments.

We note that the seismic facies of Units 2.b and 3.b shows a higher amplitude, a more pronounced lensoidal geometrical character and a restricted lateral extent (more prone to terminate against the highs) with respect to the other drift units (Fig. 6). We infer that this acoustic character suggest the occurrence of more energetic sedimentary conditions. A higher amplitude may correspond to a higher density contrast between sedimentary beds of variable mean grain size. This interpretation is also supported by the presence of normally-graded internal laying above irregular/erosive bases (e.g. cores 17612-4, 104 cm; 17614-2, 420 cm; 17619-3, 498 cm, Fig. 9). In core 17612-4 the coarser part of this graded interval contains also mud chips, supporting the hypothesis of quite energetic flows. Enhanced sediment transport could either take place in the form of downslope flow, like turbidity currents, or in the form of a more persistent sandy grain flow having a pulsing-mode supply type such as storm wave activity on the surrounding shelf banks. Such a supply could also occur in the form of suspension clouds originating on the shallow shelf and raining down over the depression as known from slope canyon systems and from shelf edges (Voigt et al., 2013; Bender et al., submitted). Alternatively, the higher density contrast between coarser and finer sediments may reflect a variation in strength of the bottom current (coarser grained sediments resulting in stronger reflections during periods of intensified velocity).

We also note that the depocenters of the main, minor and patchy, innermost drift bodies are not in a central position with respect to their lateral extents but are displaced towards the moat (Figs. 10 and 11). This is exactly what is expected in case of sediment delivery by a bottom current running inside the moat. In fact, where the bottom current is the main factor controlling sediment deposition, it is common to find the depocenter in relatively slack water next to the current axis where the sediment transport occurs (Rebesco et al., 2014a). The patchy drift in the innermost part of Kveithola Trough shows a completely transparent, condensed and mounded (not ponding, nor draping) seismic facies. These characteristics also hint to a bottom current control rather than to turbidity current or hemipelagic draping processes (Fig. 8).

We noticed that the older drift units (Units 2.a and 2.b) appear to be more affected by erosion (Fig. 6) than the overlying drift units (Units 3.a and 3.b). The lower drift units also show local sediment mounding with downlap on both opposing sides (Fig. 7). This configuration may suggest variability on the current strength and path. In particular, this configuration may indicate that the drift was more actively shaped in its earlier phase, a time with a powerful bottom current flow regime, while deposition was maintained and enhanced with continuous growing in its upper part. We hence assume that the lower part of the drift can be ascribed to the overall shaping phase and the upper drift part to the later growth phase.

The thickness of the underlying glaciomarine blanket is remarkably constant (across the whole trough) and is scarcely affected by the preconditioned morphology of the subglacial sediment underneath. This observation confirms the interpretation that these glaciomarine deposits are mainly affected by vertical settling, i.e., hemipelagic draping during open water conditions, plumite fall-out and ice-rafted debris as suggested by previous authors (Rebesco et al., 2011; Rüther et al., 2012; Bjarnadóttir et al., 2013; Lucchi et al., 2013; Hanebuth et al., 2014; Lucchi et al., 2015).

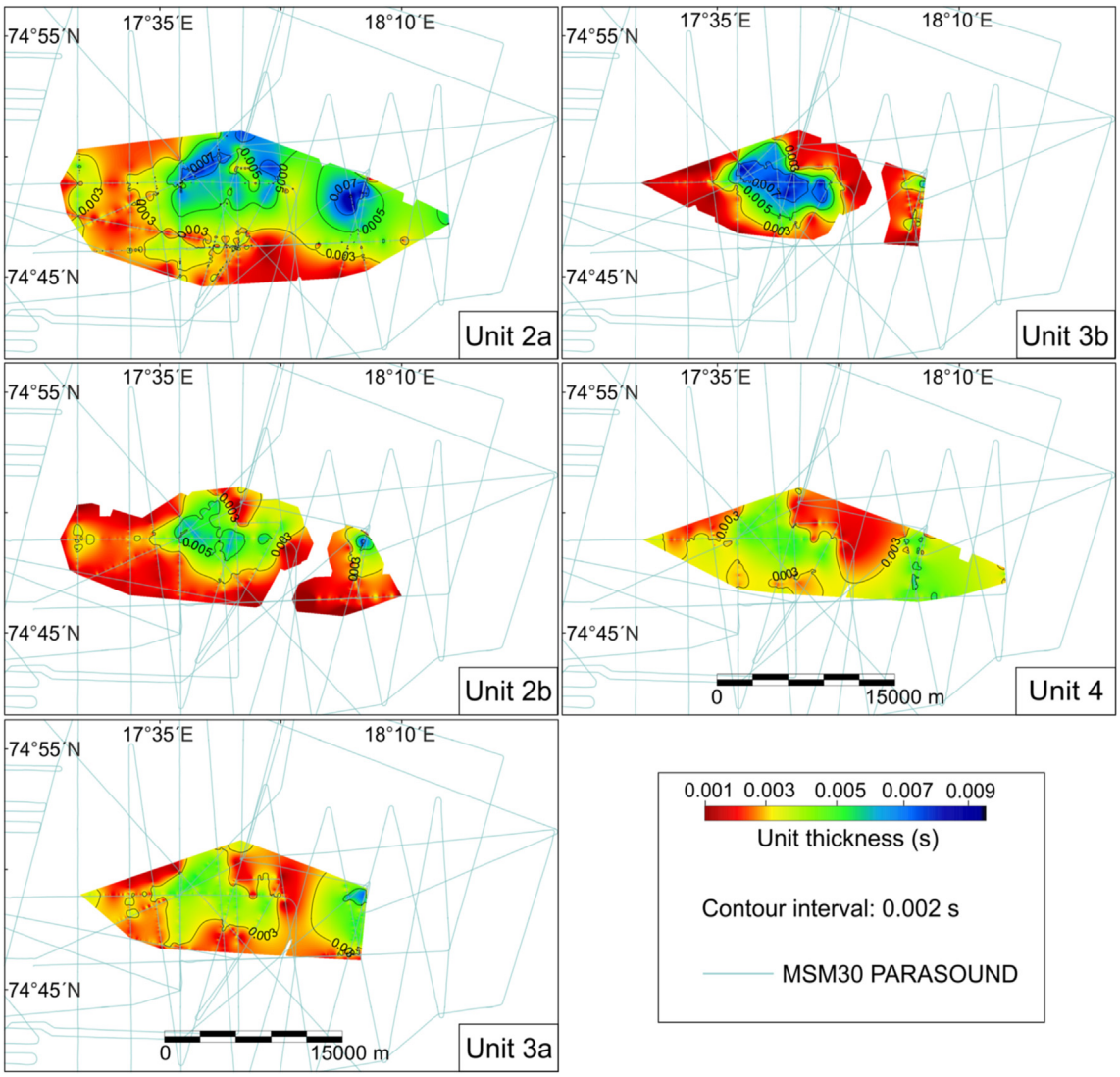

Fig. 11. Separate isochore time maps showing the sediment thickness (in seconds) of the various units of the Kveithola Drift. Location of all PARASOUND profiles acquired in the drift area during cruise MSM 30 is also shown.

7. Discussion

7.1. Water masses responsible for drift genesis

The geometry of the drift suggests a powerful bottom current on the northern side of the Kveithola Trough. Such a current may have three possible origins:

1) Atlantic Water;
2) Arctic water;
3) Brine-enriched shelf water (BSW).

1) In the first case, a branch of the West Spitsbergen Current could enter the trough from the west (Fig. 12). This scenario would be favoured by the Coriolis force pushing the current towards the right and the Atlantic water would follow the bathymetry and turn against the northern trough slope at the eastern termination of the trough. A similar process is already documented to happen in Storfjorden (e.g. Midttun, 1990; Fohrmann et al., 2001; Stiansen and Filin, 2007). In this case two opposing currents would develop on the two sides of the Kveithola Drift, as it is described for confined drifts (Faugères et al., 1999). However, on the southern edge of Kveithola Trough no moat is visible and there the sedimentary tail of Kveithola drift is relatively shallow (up to 250 m depth). This observation is not consistent with this scenario since it is difficult to envision a bottom water that does not leave any significant erosive imprint on the southern edge of the drift whereas at a few km distance it is able to generate a moat at nearly 350 m water depth on the northern edge.

2) In the second case, cold Arctic water enters the region from the northeast and reaches the eastern end of the Kveithola Trough (as documented by Stiansen and Filin, 2007). The cold Arctic water may enter the trough and follow the bathymetry. However, this water is characterized by low salinity and it is a relatively superficial water mass that by itself is not likely to sink from Spitsbergenbanken to the bottom of the Kveithola Trough and prevent deposition of sediments on the seafloor.

3) BSW is produced during winter and forms a shelf water (Aagaard et al., 1985) which accumulates in morphological depressions of the continental shelf. In due course, this dense water spills over the depressions and cascades into the regional troughs and then down the continental slope. Dense shelf water is known to

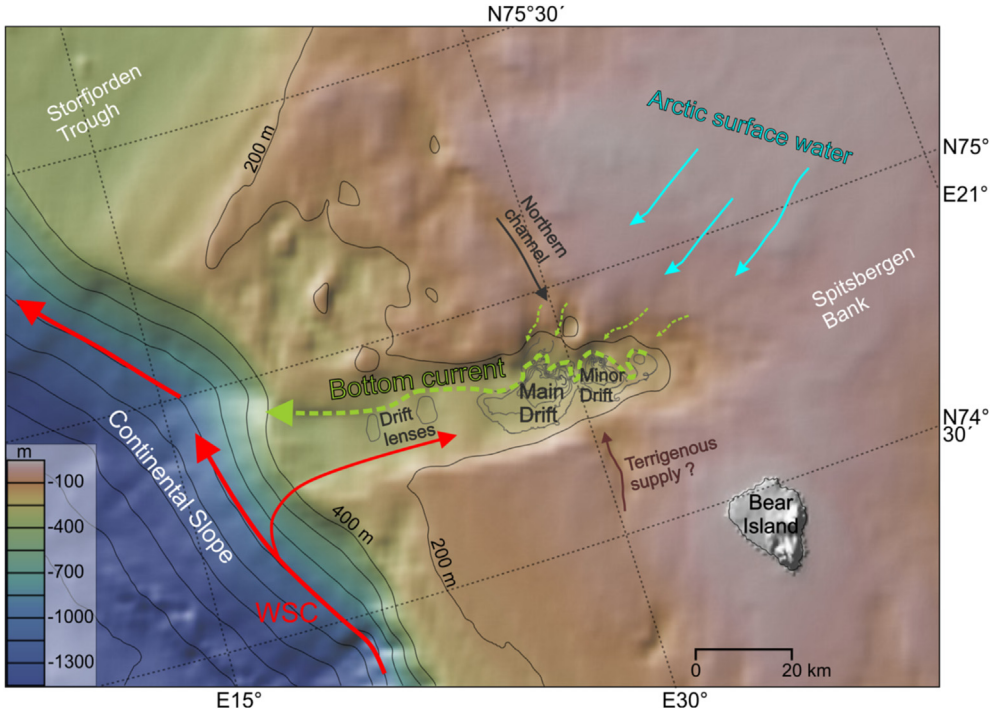

Fig. 12. Schematic diagram of the inferred currents in the Kveithola Trough area superimposed onto IBCAO bathymetry (Jakobsson et al., 2012) plotted using GeoMapApp (http://www.geomapapp.org). The contours of iso-thickness of the Kveithola Drift (every 5 ms) are also shown. A branch of the West Spitsbergen Current (WSC) (red arrow), may enter the trough, follow the bathymetry and turn west on the northern side. In light blue is the cold Arctic surface water coming from the north. Bottom current flow (green dashed arrows) within the moat to the north of the Kveithola Drift is inferred to be comprised of brine-enriched shelf water spilling from morphological shelf depressions to the north of the Kveithola Trough. A possible preferential terrigenous supply (mainly through a structurally controlled southern channel) is also shown (brown arrow). (For interpretation of the references to colour in this figure legend, the reader is referred to the web version of this article).

have the capacity to locally erode the seafloor, to transport significant amounts of sediment into the deep sea, and to lead to the formation of local depocenters (Fohrmann et al., 1998).We therefore consider it most probable that such dense water mass flow is responsible for the genesis of the Kveithola Drift and for the moat at its northern edge.

7.2. History of BSW production

The moat in the Kveithola Trough has been active since the time of Horizon 3, which defines the base of the drift. This situation suggests that the formation of BSW started around 13 cal ka BP, as determined by the oldest date from the lowest part of the drift. The same age was obtained by Rüther et al. (2012) for the onset of drift deposition. It is hence inferred that the onset of BSW production was a response to climatic forcings as the atmospheric cooling of the surface waters on the western Barents Shelf or the presence of coastal polynyas and wind influence (e.g. Skogseth et al., 2008; Wobus et al., 2013). We infer that such conditions persisted since the onset of drift deposition. BSW production could also have been somehow related to the re-establishment of the inflow of Atlantic water following the last glacial maximum. However, the shift to interglacial conditions is inferred to have occurred at 11.2 cal ka BP (Jessen et al., 2010) and brine formation is inferred to have further increased from about 8200 years BP reaching periodic maxima during the last 4000 years BP (Rasmussen and Thomsen, 2014, 2015).

Conversely, other processes seem to have prevailed prior to drift deposition when the glaciomarine drape formed (Units 1.a and 1.b). The underlying glacigenic blanket, inferred to have been deposited during the Bølling/Allerød interval (14.6–13.9 cal ka BP; Rüther et al., 2012; Bjarnadóttir et al., 2013), is assumed to be characterized by the presence of plumites and ice-rafted debris. Therefore, melt water production seems to have persisted in Kveithola pointing to ice cover on the shallow Spitsbergenbanken during that time interval.

Unit 2.b developed between 12.7 cal ka BP (the age point just below Horizon 4, Figs. 5c and 9) and 11.2 cal. ka BP (the date from the condensed succession above Horizon 4, Figs. 5c and 9). This latter age is consistent with a date of 11.2 cal ka BP obtained by Rüther et al. (2012) for the end of Drift 2 deposition, which corresponds to the overlying Horizon 5 in this study. The lower part of Unit 2.b may hence have deposited during the Younger Dryas (12.8–11.7 cal ka BP, Broecker et al., 2010), when there was an intensifying of ice conditions as documented by low primary productivity (Aagaard-Sørensen et al., 2010) and enhanced IRD supply (Slubowska-Woldengen et al., 2007). Though thermohaline circulation may have been hampered during this period by an increase in freshwater supply (Hald and Hagen, 1998; Ebbesen and Hald, 2004; Slubowska-Woldengen et al., 2007), a stronger brine formation occurred (Rasmussen and Thomsen, 2014, 2015).

We infer that more energetic sedimentary conditions were present during the development of the higher amplitude, less extensive Unit 2.b (and 3.b) with respect to the lower amplitude, more extensive Unit 2.a (and 3.a). This situation is in apparent contrast with a general reduction in bottom current activity during the Younger Dryas period (Hald and Hagen, 1998; Ebbesen and Hald, 2004; Slubowska-Woldengen et al., 2007), but is in agreement with the evidence for stronger BSW formation in the nearby Storfjorden (Rasmussen and Thomsen, 2014, 2015). The following stage of the drift (upper drift interval, Drift 2 of Bjarnadóttir et al., 2013) developed during the Pre-boreal time interval, which was characterized by a sudden rise in sea surface temperatures of the Arctic Water (Hald et al., 2007), with high primary productivity and

absence of IRD (Aagaard-Sorensen et al., 2010). In Unit 3.b, similarly to Unit 2.b, we infer more energetic sedimentary conditions (erosive/irregular surface overlain by normally graded sediments, Fig. 9). The erosive surfaces of this lithological boundary are particularly evident in the most-southerly cores (17612-4 and 17614-2). Such depositional conditions may reflect a new period of climatic deterioration. The only age we have for this unit (younger than 8.8 cal ka BP.) indicates that at least parts of the unit were deposited during the short atmospheric cooling interval of 8.8–8.2 cal ka BP, reported by Sarnthein et al. (2003). The younger Unit 4 would therefore have developed during the Holocene thermal optimum, which occurred at about 8 cal ka BP according to Hald et al., 2007.

We therefore infer that the broad variations in current regime were mainly related to fluctuations in BSW formation intensity that we assume was connected to the variations in the regional atmospheric temperature and/or presence of coastal polynyas and wind influence. However, it is also likely that changes in the intensity of BSW formation are a response to successively retreating grounded ice as well as development from perennial to seasonal sea ice conditions that allowed the stepwise establishment of initially limited, and later open, shelf current system on the western Barents shelf.

The mean winter limit of sea ice extension is controlled by the flow of Atlantic water and broadly corresponds to the position of the Polar Front. Its position in the western Barents Sea is fairly stable at present days. The fluctuations through time during the Holocene, determined by investigating past ice extents and oceanographic conditions in sedimentary records, allowed an evaluation of variations in Atlantic water inputs to the Arctic (Voronina et al., 2001). During the 11–10.5 ka BP time interval the Polar Front was located close to the Barents Sea margin and then moved eastward till 7.5 ka BP when the present-day oceanographic pattern was established (Risebrobakken et al., 2010). The mid Holocene (8–5 cal ka BP) was in general characterized by relatively warm and stable conditions. In contrast, highly variable conditions were recorded since about 5 cal ka BP, with cooler temperatures and extended sea ice cover with southward migration of the Polar Front (Voronina et al., 2001).

8. Conclusions

- We provide detailed morphological, seismostratigraphic, lithological and sedimentological insights into the construction of the Kveithola trough-confined drift. .
- This drift is characterized by a complex structure comprising a main and a minor drift bodies, two drift lenses in the outer part of the trough, a series of more or less connected drift patches in the innermost part, and small perched sediment patches in a channel to the north.
- The drift mainly shows sub-parallel reflections of good lateral continuity, an abrupt northward pinch-out forming a typical drift moat, and gradual tapering to the south.
- We identified the base of the drift and four internal horizons, defining 5 sedimentary units, which we correlated throughout the drift.
- Two units display high amplitude reflectors, a marked lensoidal character and restricted lateral extension, suggesting more energetic sedimentary conditions.
- Sedimentary cores show a facies typical for contourites with strongly bioturbated sediments, abundant silty/sandy mottles and shell fragments.
- The drift morphological and internal characteristics suggest a strong control by a bottom current flowing inside the trough, mainly along the moat at the northern edge of the drift.
- Brine-enriched shelf water (BSW) produced during the winter season is inferred to be the driver responsible for the genesis of the Kveithola Drift. The BSW flows westward along the moat before cascading the continental slope.
- The formation of BSW is inferred to have started around 13 cal ka BP, the onset of drift deposition, suggesting that atmospheric cooling of the surface waters and/or the presence of coastal polynyas and wind influence on the western Barents Shelf dominated from this time. In alternative, supercooled water masses formed below a floating ice shelf may have influenced BSW formation (Borchers et al., 2015).
- We suggest that the two units with marked lensoidal character show more energetic sedimentary conditions. Though we do not have yet conclusive dating for these units, sediment and seismic correlation suggest they date Younger Dryas and 8.8–8.2 cal ka BP respectively. This situation during cold periods is in apparent contrast with a general reduction in bottom current activity indicated by Hald and Hagen (1998), Ebbesen and Hald (2004), Slubowska-Woldengen et al. (2007), but in agreement with the evidence for stronger BSW formation in the nearby Storfjorden (Rasmussen and Thomsen, 2014, 2015).
- More detailed insight into these processes may be gained through sedimentological analysis of the available sediment cores, for which this seismostratigraphic study provides a solid framework.

Acknowledgement

The research cruise MSM30 CORIBAR and this study were partly funded through the MARUM DFG-Research Center/Cluster of Excellence “The Ocean in the Earth System” as part of MARUM project SD-2. This study contributes to the IPY initiative 367 NICESTREAM (Neogene Ice Streams and Sedimentary Processes on High- Latitude Continental Margins). The work was funded by the Italian projects OGS-EGLACOM, PNRA-CORIBAR-IT (PdR 2013/C2.01), ARCA (grant n. 25_11_2013_973) and PNRA-VALFLU, by the Council of Norway through its Centres of Excellence funding scheme (project number 223259), by the Spanish projects DEGLABAR (CTM2010-17386) and CORIBAR-ES (CTM2011-14807-E) funded by the “Ministerio de Economia y Competitividad”. The “Generalitat de Catalunya” is acknowledged for support through an excellence research group grant (2014SGR940). J.L. was funded by an FPI grant BES-2011-043614. Karen Gjertsen, Norwegian Institute of Marine Research, is thanked for having kindly provided Fig. 2. We are grate to three anonymous reviewers: this paper has been significantly improved thanks to their comments.

Appendix A. Supplementary data

Supplementary data related to this article can be found at http://dx.doi.org/10.1016/j.quascirev.2016.02.007

References

Aagaard, K., Darnall, C., Greisman, P., 1973. Year-long current measurements in the Greenland-Spitsbergen passage. Deep Sea Res. Oceanogr. Abstr. 20, 743–746.
Aagaard, K., Swift, J.H., Carmack, E.C., 1985. Thermohaline circulation in the arctic Mediterranean seas. J. Geophys. Res. 90 (C3), 4833–4846.
Aagaard, K., Foldvik, A., Hillman, S.R., 1987. The west spitsbergen current: disposition and water mass transformation. J. Geophys. Res. 92 (C4), 3778–3784.
Aagaard-Sørensen, S., Husum, K., Hald, M., Knies, J., 2010. Paleoceanographic development in the SW Barents Sea during the Late Weichselian–Early Holocene transition. Quat. Sci. Rev. 29, 3442–3456. http://dx.doi.org/10.1016/j.quascirev.2010.08.014.
Alley, R.B., Mayewski, P.A., Sowers, T., Stuiver, M., Taylor, K.C., Clark, P.U., 1997. Holocene climatic instability: a prominent, widespread event 8200 yr ago. Geology 25, 483–486.
Andreassen, K., Laberg, J.S., Vorren, T.O., 2008. Seafloor geomorphology of the SW

Barents Sea and its glaci-dynamic implications. Geomorphology 97, 157–177.
Andreassen, K., Winsborrow, M., Bjarnadóttir, L., Rüther, D., Borque, J., Lucchi, R., Caburlotto, A., 2009. Barents Sea and the West Spitsbergen Margin, UiT 2009. Marine Geophysical/Geological Cruise to Outer Bear Island trough, Kveithola trough and the West Spitsbergen Margin. Cruise Report. RV/Jan Mayen 2.-19.07.2009. University of Tromsø, p. 33.
Bender, V.B., Hanebuth, T.J.J., Nagai, R.H., submitted. Sediment export dynamics from a high-energy continental shelf as recorded on an uppermost-slope terrace (off Uruguay). Sedimentology.
Bergh, S.G., Grogan, P., 2003. Tertiary structure of the Sørkapp-Hornsund Region, South Spitsbergen, and implications for the offshore southern extension of the fold-thrust belt. Nor. J. Geol. 83, 43–60.
Bird, M.I., Austin, W.E., Wurster, C.M., Fifield, L.K., Mojtahid, M., Sargeant, C., 2010. Punctuated eustatic sea-level rise in the early mid-Holocene. Geology 38, 803–806.
Bjarnadóttir, L.R., Rüther, D.C., Winsborrow, M.C.M., Andreassen, K., 2013. Grounding-line dynamics during the last deglaciation of Kveithola, W Barents Sea, as revealed by seabed geomorphology and shallow seismic stratigraphy. Boreas 42, 84–107.
Blanchon, P., Jones, B., Ford, D.C., 2002. Discovery of a submerged relic reef and shoreline off Grand Cayman: further support for an early Holocene jump in sea level. Sediment. Geol. 147, 253–270.
Blindheim, J., 1989. Cascading of Barents Sea bottom water into the Norwegian Sea. Rapp. P. V. Réun. Cons. Int. Explor. Mer. 188, 49–58.
Bøe, R., Skardhamar, J., Rise, L., Dolan, M.F.J., Bellec, V.K., Winsborrow, M., Skagseth, T., Knies, J., King, E.L., Walderhaug, O., Chand, S., Buenz, S., Mienert, J., 2015. Sandwaves and sand transport on the Barents Sea continental slope offshore northern Norway. Mar. Pet. Geol. 60, 34–53.
Borchers, A., Dietze, E., Kuhn, G., Esper, O., Voigt, I., Hartmann, K., Diekmann, B., 2015. Holocene ice dynamics and bottom-water formation associated with Cape Darnley Polynya activity recorded in Burton Basin, East Antarctica. Mar. Geophys. Res. http://dx.doi.org/10.1007/s11001-015-9254-z (in press).
Boyd, T.J., D'Asaro, E.A., 1994. Cooling of the West Spitsbergen current - wintertime observations west of Svalbard. J. Geophys. Res. 99 (C11), 22597–22618.
Broecker, W.S., Denton, G.H., Edward, R.L., Cheng, H., Alley, R.B., 2010. Putting the Younger Dryas cold event into context. Quat. Sci. Rev. 29, 1078–1081.
Camerlenghi, A., Flores, J.A., Sierro, F.J., Colmenreo, E., the SVAIS scientific and technical staff, 2007. SVAIS, the Development of an Ice Stream-dominated Sedimentary System: the Southern Svalbard Continental Margin. Cruise report. University of Barcelona, p. 62.
Camerlenghi, A., Rebesco, M., Accettella, D., 2016. Storfjorden Trough-Mouth Fan, Barents Sea margin. In: Dowdeswell, J.A., Canals, M., Jakobsson, M., Todd, B.J., Dowdeswell, E.K., Hogan, K.A. (Eds.), Atlas of Submarine Glacial Landforms: Modern, Quaternary and Ancient, Geological Society of London Memoirs Series 46 (in press).
Deschamps, P., Durand, N., Bard, E., Hamelin, B., Camoin, G., Thomas, A.L., Henderson, G.M., Okuno, J., Yokoyama, Y., 2012. Ice-sheet collapse and sea-level rise at the Bølling warming 14,600 years ago. Nature 483, 559–564.
Ebbesen, H., Hald, M., 2004. Unstable Younger Dryas climate in the northeast North Atlantic. Geology 32, 673–676.
Faugères, J.-C., Stow, D.A.V., Imbert, P., Viana, A.R., 1999. Seismic features diagnostic of contourite drifts. Mar. Geol. 162, 1–38.
Fohrmann, H., Backhaus, J.O., Blaume, F., Rumohr, J., 1998. Sediments in bottom-arrested gravity plumes: numerical case studies. J. Phys. Oceanogr. 28, 2250–2274.
Fohrmann, H., Backhaus, J.O., Blaume, F., Haupt, B.J., Kämpf, J., Michels, K., Mienert, J., Posewang, J., Ritzrau, W., Rumohr, J., Weber, M., Woodgate, R., 2001. Modern ocean current-controlled sediment transport in the Greenland-Iceland-Norwegian (GIN) seas. In: Schäfer, P., Ritzrau, W., Schlüter, M., Thiede, J. (Eds.), The Northern North Atlantic. Springer Berlin Heidelberg, pp. 135–154.
Gabrielsen, R.H., Færseth, R.B., Jensen, L.N., Kalheim, J.E., Riis, F., 1990. Structural elements of the Norwegian continental shelf, part I: the Barents Sea region. Nor. Pet. Dir. Bull. 6, 33.
Grave, M., 2014. Structure and Formation of Shallow Water Contourites - Geophysical and Sedimentological Analysis of the Drift inside the Kveithola trough, Western Barents Sea. Master Thesis M.Sc. "Geowissenschaften". Department of Geosciences, University of Bremen, p. 58.
Hald, M., Hagen, S., 1998. Early preboreal cooling in the Nordic seas region triggered by melt water. Geology 26, 615–618.
Hald, M., Andersson, C., Ebbesen, H., Jansen, E., Klitgaard-Kristensen, D., Risebrobakken, B., Salomonsen, G.R., Sarnthein, M., Sejrup, H.P., Telford, R.J., 2007. Variations in temperature and extent of Atlantic Water in the northern North Atlantic during the Holocene. Quat. Sci. Rev. 26, 3423–3440. http://dx.doi.org/10.1016/j.quascirev.2007.10.005.
Hanebuth, T.J., Bergenthal, M., Caburlotto, A., Dippold, S., Düßmann, R., Freudenthal, T., Hörner, T., Kaszemeik, K., Klar, S., Lantzsch, H., Llopart, J., Lucchi, R.G., Nicolaisen, L.S., Noorlander, K., Osti, G., Özmaral, A., Rebesco, M., Rosiak, U., Sabbatini, A., Schmidt, W., Stachowski, A., Urgeles, R., 2013. CORIBAR – Ice Dynamics and Meltwater Deposits: Coring in the Kveithola Trough, NW Barents Sea. Cruise MSM30. In: Berichte, MARUM – Zentrum fur Marine Umweltwissenschaften, FachbereichGeowissenschaften, 299. Universität Bremen, Bremen, p. 74. ISSN 2195–7894.
Hanebuth, T.J., Rebesco, M., Urgeles, R., Lucchi, R.G., Freudenthal, T., 2014. Drilling glacial deposits in offshore polar regions. Eos 95, 277–278.
Hanebuth, T.J., Zhang, W., Hofmann, A.L., Löwemark, L.A., Schwenk, T., 2015. Oceanic density fronts steering bottom-current induced sedimentation deduced from a 50 ka contourite-drift record and numerical modeling (off NW Spain). Quat. Sci. Rev. 112, 207–225.
Jakobsson, M., Mayer, L., Coakley, B., Dowdeswell, J.A., Forbes, S., Fridman, B., Hodnesdal, H., Noormets, R., Pedersen, R., Rebesco, M., Schenke, H.W., Zarayskaya, Y., Accettella, D., Armstrong, A., Anderson, R.M., Bienhoff, P., Camerlenghi, A., Church, I., Edwards, M., Gardner, J.V., Hall, J.K., Hell, B., Hestvik, O., Kristoffersen, Y., Marcussen, C., Mohammad, R., Mosher, D., Nghiem, S.V., Pedrosa, M.T., Travaglini, P.G., Weatherall, P., 2012. The International Bathymetric chart of the Arctic Ocean (IBCAO) version 3.0. Geophys. Res. Lett. 39, L12609.
Jessen, S.P., Rasmussen, T.L., Nielsen, T., Solheim, A., 2010. A new Late Weichselian and Holocene marine chronology for the western Svalbard slope 30,000–0 cal years BP. Quat. Sci. Rev. 29, 1301–1312.
Jungclaus, J.H., Backhaus, J.O., Fohrmann, H., 1995. Outflow of dense water from the Storfjord in Svalbard: a numerical model study. J. Geophys. Res. 100 (C12), 24719–24728.
King, E.L., Bøe, R., Bellec, V.K., Rise, L., Skardhamar, J., Ferré, B., Dolan, M.F.J., 2014. Contour current driven continental slope-situated sandwaves with effects from secondary current processes on the Barents Sea margin offshore Norway. Mar. Geol. 353, 108–127.
Laberg, J.S., Andreassen, K., Vorren, T.O., 2012. Late Cenozoic erosion of the high-latitude southwestern Barents Sea shelf revisited. Geol. Soc. Am. Bull. 124, 77–88.
Lebesbye, E., Vorren, T.O., 1996. Submerged terraces in the southwestern Barents Sea: origin and implications for the late Cenozoic geological history. Mar. Geol. 130, 265–280.
Llopart, J., Urgeles, R., Camerlenghi, A., Lucchi, R.G., Rebesco, M., De Mol, B., 2015. Late Quaternary development of the Storfjorden and Kveithola Trough Mouth Fans, northwestern Barents Sea. Quat. Sci. Rev. 129, 68–84.
Lucchi, R.G., Camerlenghi, A., Rebesco, M., Urgeles, R., Sagnotti, L., Macri, P., Colmenero-Hildago, E., Sierro, F.J., Melis, R., Morigi, C., Barcena, M.A., Giorgetti, G., Villa, G., Persico, D., Flores, J.A., Pedrosa, M.T., Caburlotto, A., 2013. Postglacial sedimentary processes on the Storfjorden and Kveithola trough-mouth fans: impact of extreme glacimarine sedimentation. Glob. Planet. Change 111, 309–326.
Lucchi, R.G., Sagnotti, L., Camerlenghi, A., Macrì, P., Rebesco, M., Pedrosa, M.T., Giorgetti, G., 2015. Marine sedimentary Record of Meltwater Pulse 1a in the NW Barents Sea Continental Margin. αrktos, 1 online. http://link.springer.com/article/10.1007/s41063-015-0008-6.
Mangerud, J., Gulliksen, S., 1975. Apparent radiocarbon ages of recent marine shells from Norway, Spitsbergen, and Arctic Canada. Quat. Res. 5, 263–273.
Midttun, L., 1990. Surface temperatures of the Barents Sea. Polar Res. 8, 11–16.
Müller-Michaelis, A., Uenzelmann-Neben, G., 2015. Using seismic reflection data to reveal high-resolution structure and pathway of the upper Western Boundary undercurrent core at Eirik Drift. Mar. Geophys. Res. http://dx.doi.org/10.1007/s11001-015-9255-y (in press).
Pedrosa, M., Camerlenghi, A., De Mol, B., Urgeles, R., Rebesco, M., Lucchi, R.G., 2011. SVAIS and EGLACOM Cruises shipboard parties, Seabed Morphology and Shallow Sedimentary Structure of the Storfjorden and Kveitehola Trough-Mouth Fans (north west Barents Sea). Mar. Geol. 286, 65–81.
Poulain, P.-M., Warn-Varnas, A., Niiler, P.P., 1996. Near surface circulation of the Nordic Seas as measured by Lagrangian Drifters. J. Geophys. Res. 101 (C8), 18237–18258.
Quadfasel, D., Rudels, B., Kurz, K., 1988. Outflow of dense water from a Svalbard fjord into the Fram Strait. Deep Sea Res. 35, 1143–1150.
Rasmussen, T.L., Thomsen, E., Slubowska, M.A., Jessen, S., Solheim, A., Koç, N., 2007. Paleoceanographic evolution of the SW Svalbard margin (76°N) since 20,000 ^{14}C yr BP. Quat. Res. 67, 100–114.
Rasmussen, T.L., Thomsen, E., 2014. Brine formation in relation to climate changes and ice retreat during the last 15,000years in Storfjorden, Svalbard, 76-78N. Paleoceanography 29, 911–929.
Rasmussen, T.L., Thomsen, E., 2015. Palaeoceanographic development in Storfjorden, Svalbard, during the deglaciation and Holocene: evidence from benthic foraminiferal records. Boreas 44, 24–44.
Rebesco, M., Stow, D., 2001. Seismic expression of contourites and related deposits: a preface. In: Rebesco, M., Stow, D.A.V. (Eds.), Seismic Expression of Contourites and Related Deposits, Marine Geophys. Res., vol. 22, pp. 303–308.
Rebesco, M., 2005. Contourites. In: Richard, C., Selley, R.C., Cocks, L.R.M., Plimer, I.R. (Eds.), Encyclopedia of Geology, vol. 4. Elsevier, Oxford, pp. 513–527.
Rebesco, M., Camerlenghi, A., Van Loon, A.J., 2008. Preface. In: Rebesco, M., Camerlenghi, A. (Eds.), Contourites, Developments in Sedimentology, 60, pp. xvii–xviii.
Rebesco, M., Liu, Y., Camerlenghi, A., Winsborrow, M., Laberg, J.S., Caburlotto, A., Diviacco, P., Accettella, D., Sauli, C., Tomini, I., Wardell, N., 2011. Deglaciation of the Barents Sea Ice Sheet - a swath bathymetric and sub-bottom seismic study from the Kveitehola Trough. Mar. Geol. 279, 141–147.
Rebesco, M., Wåhlin, A., Laberg, J.S., Schauer, A., Brezcynska-Möller, A., Lucchi, R.G., Noormets, R., Accettella, D., Zarayskaya, Y., Diviacco, P., 2013. Quaternary contourite drifts of the Western Spitsbergen margin. Deep Sea Res. Part I 79, 156–168.
Rebesco, M., Hernández Molina, J., van Rooij, D., Wåhlin, A., 2014a. Contourites and associated sediments controlled by deep-water circulation processes: state-of-the-art and future considerations. Mar. Geol. 352, 111–154.
Rebesco, M., Laberg, J.S., Pedrosa, M.T., Camerlenghi, A., Lucchi, R.G., Zgur, F.,

Wardell, N., 2014b. Onset and growth of Trough-Mouth Fans on the North-Western Barents Sea margin – implications for the evolution of the Barents Sea/Svalbard Ice Sheet. Quat. Sci. Rev. 92, 227–234.
Rebesco, M., Urgeles, R., Özmaral, A., CORIBAR Scientific Party, 2016. Grounding Zone Wedges and mega-scale glacial lineations in Kveithola Trough, NW Barents Sea. In: Dowdeswell, J.A., Canals, M., Jakobsson, M., Todd, B.J., Dowdeswell, E.K., Hogan, K.A. (Eds.), Atlas of Submarine Glacial Landforms: Modern, Quaternary and Ancient. Geological Society of London, Memoirs Series 46 (in press).
Reimer, P.J., Bard, E., Bayliss, A., Beck, J.W., Blackwell, P.G., Bronk Ramsey, C., Buck, C.E., Cheng, H., Edwards, R.L., Friedrich, M., Grootes, P.M., Guilderson, T.P., Haflidason, H., Hajdas, I., Hatté, C., Heaton, T.J., Hogg, A.G., Hughen, K.A., Kaiser, K.F., Kromer, B., Manning, S.W., Niu, M., Reimer, R.W., Richards, D.A., Scott, E.M., Southon, J.R., Turney, C.S.M., van der Plicht, J., 2013. IntCal13 and MARINE13 radiocarbon age calibration curves 0–50000 years cal BP. Radiocarbon 55, 1869–1887. http://dx.doi.org/10.2458/azu_js_rc.55.16947.
Risebrobakken, B., Moros, M., Ivanova, E.V., Chistyakova, N., Rosenberg, R., 2010. Climate and oceanographic variability in the SW Barents Sea during the Holocene. Holocene 20, 609–621.
Rudels, B., Quadfasel, D., 1991. Convection and deep water formation in the Arctic Ocean-Greenland Sea System. J. Mar. Syst. 2, 435–450.
Rüther, D.C., Bjarnadóttir, L.R., Junttila, J., Husum, K., Rasmussen, T.L., Lucchi, R.G., Andreassen, K., 2012. Pattern and timing of the north-western Barents Sea Ice Sheet deglaciation and indications for episodic Holocene deposition. Boreas 41, 494–512.
Sarnthein, M., Pflaumann, U., Weinelt, M., 2003. Past extent of sea ice in the northern North Atlantic inferred from foraminiferal paleotemperature estimates. Paleoceanography 18, 25–1.
Schauer, U., 1995. The release of brine-enriched shelf water from Storfjord into the Norwegian Sea. J. Geophys. Res. 100 (C8), 16015–16028.
Skogseth, R., Smedsrud, L.H., Nilsen, F., Fer, I., 2008. Observations of hydrography and downflow of brine-enriched shelf water in the Storfjorden polynya. Svalbard. J. Geophys. Res. (Oceans) 113, C08049.
Slubowska-Woldengen, M., Rasmussen, T.L., Koc, N., Klitgaard-Kristensen, D., Nilsen, F., Solheim, A., 2007. Advection of Atlantic water to the western and northern Svalbard shelf since 17,500 cal yr B.P. Quat. Sci. Rev. 26, 463–478.
Slubowska-Woldengen, M., Koç, N., Rasmussen, T.L., Klitgaard-Kristensen, D., Hald, M., Jennings, A.E., 2008. Time-slice reconstructions of ocean circulation changes on the continental shelf in the Nordic and Barents Seas during the last 16,000 cal yr B.P. Quat. Sci. Rev. 27, 1476–1492.
Stiansen, J.E., Filin, A.A. (Eds.), 2007. Joint PINRO/IMR Report on the State of the Barents Sea Ecosystem 2006, with Expected Situation and Considerations for Management, p. 209. IMR/PINRO Joint Report Series No. 2. ISSN 1502-8828.
Stow, D.A.V., Pudsey, C.J., Howe, J.A., Faugères, J.-C., Viana, A.R. (Eds.), 2002. Deep-water Contourite Systems: Modern Drifts and Ancient Series, Seismic and Sedimentary Characteristics. Geological Society. London, Memoirs, 22.
Stow, D.A.V., Faugères, J.-C., 2008. Contourite facies and facies model. In: Rebesco, M., Camerlenghi, A. (Eds.), Contourites, Developments in Sedimentology, 60, pp. 223–250.
Stuiver, M., Reimer, P.J., 1993. Extended 14C database and revised CALIB radiocarbon calibration program. Radiocarbon 35, 215–230.
Telford, R.J., Heegaard, E., Birks, H.J.B., 2004. The intercept is a poor estimate of a calibrated radiocarbon age. Holocene 14, 296–298.
Thomsen, C., Blaume, F., Fohrmann, H., Peeken, I., Zeller, U., 2001. Particle transport processes at slope environments—event driven flux across the Barents Sea continental margin. Mar. Geol. 175, 237–250.
van Weering, T., Stoker, M.S., Rebesco, M., 2008. High-latitude contourites. In: Rebesco, M., Camerlenghi, A. (Eds.), Contourites, Developments in Sedimentology, 60, pp. 457–489.
Voelker, A.H.L., Lebreiro, S.M., Schonfeld, J., Cacho, I., Erlenkeuser, H., Abrantes, F., 2006. Mediterranean outflow strengthening during northern hemisphere coolings: a salt source for the glacial Atlantic? Earth Planet. Sc. Lett. 245, 39–55.
Voigt, I., Henrich, R., Preu, B., Piola, A.R., Hanebuth, T.J.J., Schwenk, T., Chiessi, C.M., 2013. A submarine canyon as climatic archive – interaction of the Antarctic intermediate Water with the Mar del Plata Canyon (Southwest Atlantic). Mar. Geol. 341, 46–57.
Voronina, E., Polyak, L., de Vernal, A., Peyron, O., 2001. Holocene variations of sea-surface conditions in the southeastern Barents Sea reconstructed from dinoflagellate cyst assemblages. J. Quat. Sci. 16, 717–726.
Vorren, T.O., Laberg, J.S., 1996. Late glacial air temperature, oceanographic and ice sheet interactions in the southern Barents Sea region. In: Andrews, J.T., Austin, W.E.N., Bergsten, H., Jennings, A.E. (Eds.), Late Quaternary Palaeoceanography of the North Atlantic Margins, Special Publication No. 111. Geological Society, London, pp. 303–321.
Wobus, F., Shapiro, G.I., Huthnance, J.M., Maqueda, M.A.M., 2013. The piercing of the Atlantic layer by an Arctic shelf water cascade in an idealised study inspired by the Storfjorden overflow in Svalbard. Ocean. Model. 71, 54–65.
Zgur, F., Caburlotto, A., Deponte, D., De Vittor, C., De Vittor, R., Facchin, L., Pelos, C., Tomini, I., Rebesco, M., 2008. EGLACOM, Evolution of a GLacial Arctic COntinental Margin: the Southern Svalbard Ice Stream - Dominated Sedimentary System. Cruise Report, p. 88. REL. OGS 2008/111. OGS, Trieste.